Investigation of the Thermodynamics of Carbon Dioxide and Methane Adsorption on Various Aerogels

By

Muhammad Anas

A Dissertation Submitted to the Graduate School of Sciences and Engineering in Partial Fulfillment of the Requirements for the Degree of

Master of Science

in

Chemical and Biological Engineering

KOÇ UNIVERSITY

June 09, 2017

Investigation of the Thermodynamics of Carbon Dioxide and Methane Adsorption on Various Aerogels

Koç University

Graduate School of Sciences and Engineering

This is to certify that I have examined this copy of a master's thesis by

Muhammad Anas

and have found that it is complete and satisfactory in all respects, and that any and all revisions required by the final examining committee have been made.

Committee Members:

_____

Can Erkey, Ph.D. (Advisor)

_____

Seda Keskin Avcı, Ph.D.

_____

Ayşe Bayrakçeken Yurtcan, Ph.D.

Date: June 16, 2017

Dedicated to my parents

ABSTRACT

Thermodynamics of carbon dioxide and methane adsorption on various aerogels was investigated to evaluate their potential as adsorbents for carbon dioxide capture and methane storage. Excess CO_2 and CH_4 adsorption isotherms on aerogels such as silica, resorcinol-formaldehyde, carbon and wheat starch were measured using a volumetric method in the temperature range of 298-328 K and pressures up to 120 bar. Total or absolute adsorption isotherms were calculated from experimentally obtained excess adsorption isotherms using the pore volume of each adsorbent. It was determined that silica aerogel had maximum absolute CO_2 uptake of 14 mmol/g at 308 K and 35 bar and resorcinol-formaldehyde aerogel (RFA-17) had maximum absolute CH_4 uptake of 22 mmol/g at 298 K and 100 bar. CO_2 and CH_4 adsorption isotherms for silica aerogel were well represented with the Langmuir model. CO_2 isotherms for resorcinol-formaldehyde, carbon and wheat starch aerogel and CH_4 isotherms for carbon and resorcinol-formaldehyde aerogels were fitted with the Freundlich model. It was also found that the excess CO_2 uptake correlated well with the mesopore surface area of each aerogel at various pressures while micropore surface area significantly influenced CH_4 uptake in aerogels. The isosteric heat of adorption for each aerogel was also determined from the variation of pressure with temperature at a constant excess uptake and was found to be dependent on the surface coverage. Among all aerogels, wheat starch aerogel had highest heats of CO_2 adsorption and resorcinol-formaldehyde aerogel had highest heats of CH_4 adsorption. Adsorption capacities of aerogels determined were comparable with other classes of adsorbents and presents an opportunity for further investigation of aerogels as potential materials for applications in carbon dioxide capture and methane storage.

ÖZET

Karbon dioksit ve metanın çeşitli aerojeller üzerine adzorpsiyonunun termodinamiği araştırılmıştır. Silika, rezorsinol-formaldehit, karbon ve buğday nişastası gibi çeşitli aerojellerin CO_2 ve CH_4 adzorpsiyon izotermleri 298-328 K sıcaklık aralığında ve 120 bara kadar hacimsel yöntem kullanılarak ölçülmüştür. Aşırı adzorpsiyon izotermleri deneysel olarak ölçülüp, mutlak adzorpsiyon izotermleri adzorbanların gözenek hacimlerini kullanarak hesaplanmıştır. Silika aerojelin 308 K ve 35 bardaki maksimum mutlak CO_2 adszrpsiyonu 14 mmol/g olarak bulunmuş, rezorsinol-formaldehit aerojelin (RFA-17) 298 K ve 100 bardaki maksimum mutlak CH_4 adsorpsiyonu 22 mmol/g olarak belirlenmiştir. Silika aerojelin CO_2 ve CH_4 adzorpsiyon izotermleri Langmuir modeli ile uyumlu bulunmuştur. Rezorsinol-formaldehit, karbon ve buğday nişastası aerojellerin CO_2 adzorpsiyon izotermleri ve karbon ve rezorsinol-formaldehit aerojellerin CH_4 izotermleri Freundlich modeli ile uyumlu bulunmuştur. Bu da CH_4 adzorpsiyonun önemli derecede aerojel mikropor yüzey alanına bağlı olduğunu göstermiştir. Çeşitli basınçlarda CO_2 adzorpsiyonunun aerojelin mezopor yüzey alanıyla doğrudan ilişkili olduğu bulunmuştur. Sabit aşırı alımda aerojellerin izosterik adzorpsiyon ısıları belirlenmiş ve izosterik adzorpsiyon ısısının yüzeye adzorplanan miktara bağlı olduğu anlaşılmıştır. Tüm aerojeller arasında buğday nişastasından yapılan aerojel en yüksek izosterik adzorpsiyon ısısına sahipken, resorsinol-formaldehit aerojelin en yüksek CH_4 adsorpsiyon ısısına sahip olduğu görülmüştür. Aerojellerin adzorpsiyon kapasiteleri diğer adzorban maddeler ile karşılaştırılmış ve aerojellerin CO_2 ve CH_4 yakalama alanında umut verici malzemeler olduğu anlaşılmıştır.

ACKNOWLEDGEMENTS

I am grateful to my mentor, teacher, and thesis advisor Professor Dr. Can Erkey for providing me the opportunity to work under his supervision during my graduate studies. It was a remarkable experience to learn and develop new skills under his guidance and his support and patience during this process cannot be stated in words.

I am very thankful to my thesis review committee members Dr. Seda Keskin and Dr. Ayşe Bayrakçeken for taking their valuable time out to review this document.

I would also like to thank Arçelik, Koç University, and Nanohybrids Horizon 2020 for funding my projects during the graduate studies.

Lastly, I am thankful to my family, friends, and colleagues for their support in making this accomplishment possible.

TABLE OF CONTENTS

LIST OF TABLES

LIST OF FIGURES

NOMENCLATURE

q	*Amount adsorbed in mmol.g^{-1}*
K	*Langmuir constant bar^{-1}*
q_m	*Maximum amount adsorbed in mmol.g^{-1}*
P	*Equilibrium pressure in bar*
P_o	*Saturation pressure in bar*
E_1	*Heat of adsorption of first layer in kJ.mol^{-1}*
E_L	*Heat of adsorption of second and higher layers in kJ.mol^{-1}*
R	*Molar gas constant in J.K^{-1}.mol^{-1}*
T	*Temperature in K*
K_f	*Freundlich parameter*
n	*Heterogenity parameter*
Q_{st}	*Isosteric heat of adsorption in kJ.mol^{-1}*
Γ_{excess}	*Excess adsorbed amount in mmol.g^{-1}*
z	*Distance in m*
ρ	*Density of the adsorbate in mmol.cm^{-3}*
ρ_{bulk}	*Density of the bulk phase in mmol.cm^{-3}*
$\Gamma_{absolute}$	*Absolute adsorbed amount in mmol.g^{-1}*
ρ_{fluid}	*Molar density of the fluid mmol.cm^{-3}*
V_{pore}	*Pore Volume in cm^3.g^{-1}*
V_{ads}	*Volume adsorbed in cm^3.g^{-1}*
ρ_{ads}	*Molar density of the adsorbed phase in mmol.cm^{-3}*
b	*van der Waal's constant*
R^2	*Correlation coefficient*

1. INTRODUCTION

Total world consumption of energy is predicted to increase by 48% from 2012 to 2040 with 78% of energy being supplied by coal, oil and natural gas [1]. This increased usage of carbon based fuels would affect the rate of climate change. Therefore, there is a need to develop efficient and cost-effective systems to help prevent the increase of concentration of greenhouse gases in the atmosphere. In addition, there is also a need to have systems that can increase the relative usage of natural gas to coal and oil because of the clean burning properties of natural gas as well as having 40% less greenhouse emissions compared to coal and oil [1].

Adsorption based systems are attracting considerable attention for tackling energy and environmental issues due to being applicable in the wide range of temperature and pressure and requiring less energy for operation [2]. These systems use different types of materials as adsorbents such as metal oxides, activated carbon, zeolites, metal organic frameworks (MOFs) and aerogels [3]. The properties of adsorbents could be tailored during synthesis to satisfy the requirements for a specific application. All types of adsorbents are being investigated for applications in carbon dioxide (CO_2) capture and natural gas (CH_4) storage [3, 4], however, supercritically-dried aerogels may have significant potential to be used as adsorbents for carbon dioxide capture and methane storage.

Aerogels are mesoporous materials prepared via sol-gel method and supercritical extraction of the solvent from the pores using carbon dioxide. Different aerogels such as silica, carbon, resorcinol-formaldehyde and alginate aerogels are being synthesized and tested for adsorption, thermal insulation and drug delivery applications due to their high surface areas and tunable properties [5, 6]. Many studies report carbon dioxide adsorption

on aerogels, however there are no studies on organic aerogels and adsorption of carbon dioxide and methane on aerogels up to high pressures. There are also no systematic study on the effect of surface and pore properties on CO_2 and CH_4 adsorption.

For adsorption applications, adsorption isotherm is an important thermodynamic equilibrium relationship showing the amount of gas adsorbed on an adsorbent as a function of pressure at a constant temperature. This relationship is important for several reasons such as determining the performance of an adsorbent for specific application, evaluating thermodynamic properties such as heats of adsorption, and helping in designing and modelling of adsorption systems [7]. Isotherms determined experimentally provide excess uptakes and to accurately design adsorption systems, it is important to take total or absolute adsorption into account by considering the volume of adsorbate inside the pores of the adsorbent.

In this study, we synthesized various organic and inorganic aerogels and measured excess CO_2 and CH_4 adsorption isotherms at three different temperatures up to pressures of 120 bar. We also calculated heats of adsorption for all aerogels at different values of adsorbed amounts. In order to accurately determine potential of aerogels as adsorbents for CO_2 capture and CH_4 storage, we also calculated absolute adsorption and compared the results with other promising adsorbents for similar applications.

In this document, a brief review of adsorption thermodynamics and aerogels is provided in Chapter 2. Chapter 3 outlines the experimental methods used including the synthesis of aerogels and measurements and calculation of adsorption isotherms. Chapter 4 covers the results obtained and provides comparison of aerogels performance with other adsorbents. Chapter 5 summarizes the project and provides future directions.

2. LITERATURE REVIEW

2.1. Adsorption

Adsorption is the interaction of gas molecules with the solid. The gas which is capable of being adsorbed is called adsorbate and the solid material which is a source of the active sites responsible for the interaction with the gas is known as the adsorbent [8]. Figure 1 shows the adsorption process happening at the surface of the solid. Two types of active sites are responsible for adsorption. Gas molecules can either adsorb on the surface of the solid or the surface of other already adsorbed gas molecules. The reverse of adsorption process is known as desorption.

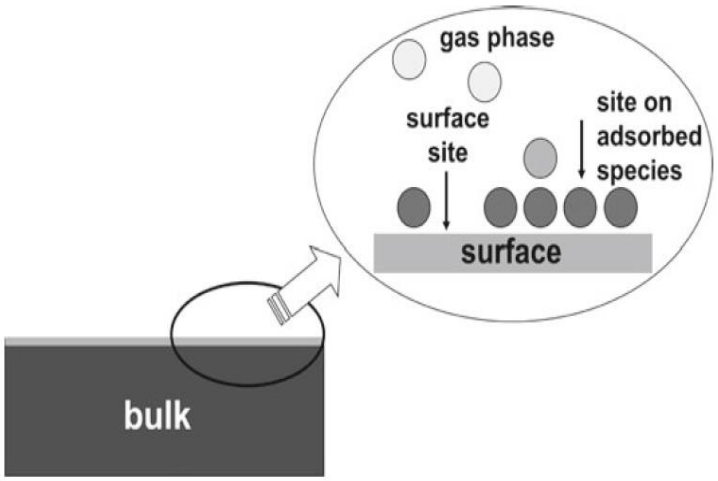

Figure 1. Adsorption Process at the Surface of an Adsorbent [8]

Adsorption process is called physisorption when the interactions are due to the result of physical forces such as van der Waaal's forces or hydrogen bond. On the other hand, chemisorption is when the interaction is via a chemical reaction [8]. Adsorption does not only occur at the solid-gas interface but could also take place at the liquid-gas, liquid-liquid and solid-liquid interfaces. However, applications of adsorption is focused more on the solid-gas interface and the research in this area is significant compared to others [9].

2.2. Thermodynamics of Adsorption

When a gas is trapped in a container with an adsorbent, the pressure of the gas will decrease and the weight of the adsorbent will increase. These changes signify the process of adsorption. A thermodynamic equilibirum is reached when the pressure and the weight do not change anymore. This equilibrium can be quantified and is helpful in the development of adsorption systems [8, 10].

2.2.1. Adsorption Isotherms

Isotherms are equilibrium relationship between the amount of gas adsorbed and the pressure at a constant temperature. There are six types of isotherms according to Brunauer classification [11] and Figure 2 shows these types of isotherms.

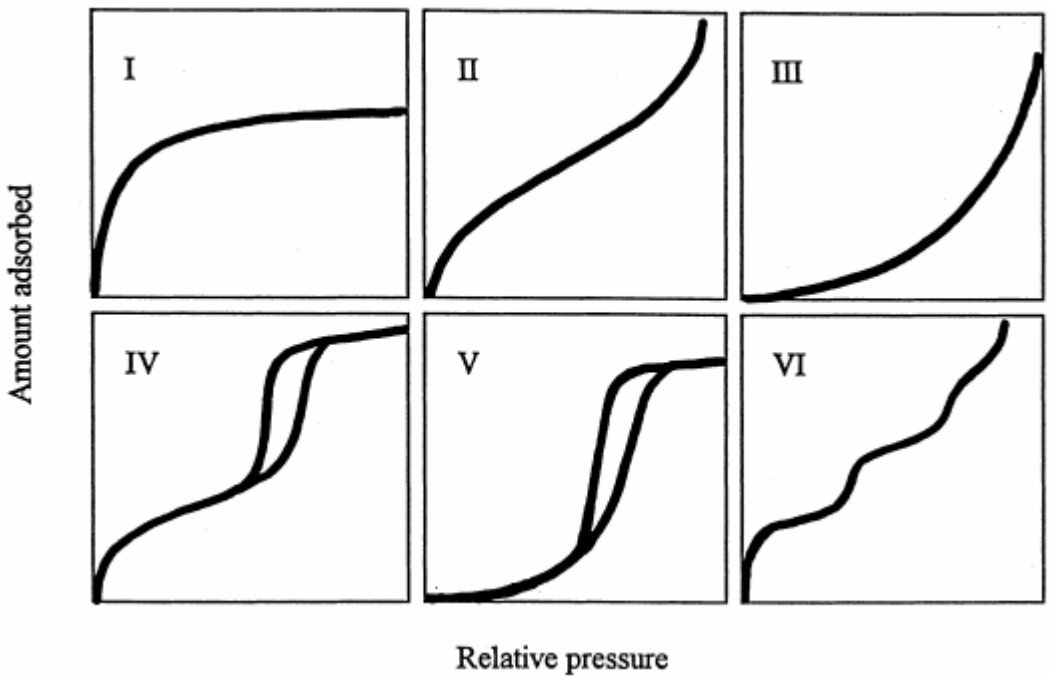

Figure 2. Brunauer Classification of Isotherms [11]

The shape of an isotherm is a result of the difference in adsorbent-adsorbate interaction due to the different sizes of pores in the adsorbent [12]. According to the IUPAC classification, adsorbent is micorporous if it has pores of less than 2 nm sizes, mesoporous if the pore size is between 2 nm and 50 nm and macroporous if the pore size

is greater than 50 nm [13]. Type I isotherm reflects adsorption process with few molecular layers on the adsorbent. Type II is indicative of macroporous adsorbent while Type III shows an unfavorable isotherm with weak adsorbent-adsorbate interaction. Type IV and V show hysteris which is common in mesoporous materials with Type V reflecting weak interactions. Type VI is rare and different steps are due to multilayer adsorption on a nonporous adsorbent [8, 12].

2.2.2. Techniques to Measure Isotherms

Different methods have been developed to measure isotherms accurately. Gravimetric methods measure the change in weight of the adsorbent [14] and volumetric methods measure the volume of gas adsorbed [15]. Both static and dynamic modes are available for gravimetric and volumetric methods. Spectroscopic methods are also being used in which the the amount adsorbed is related to IR absorbance of adsorbed species [16]. Molecular simulations have also attracted attention to theoretically calculate isotherms in order to avoid expensive experimental setup and provide comparison to experimental results [17]. Figure 3 and Figure 4 show the schematics of static gravimetric and volumetric methods, respectively.

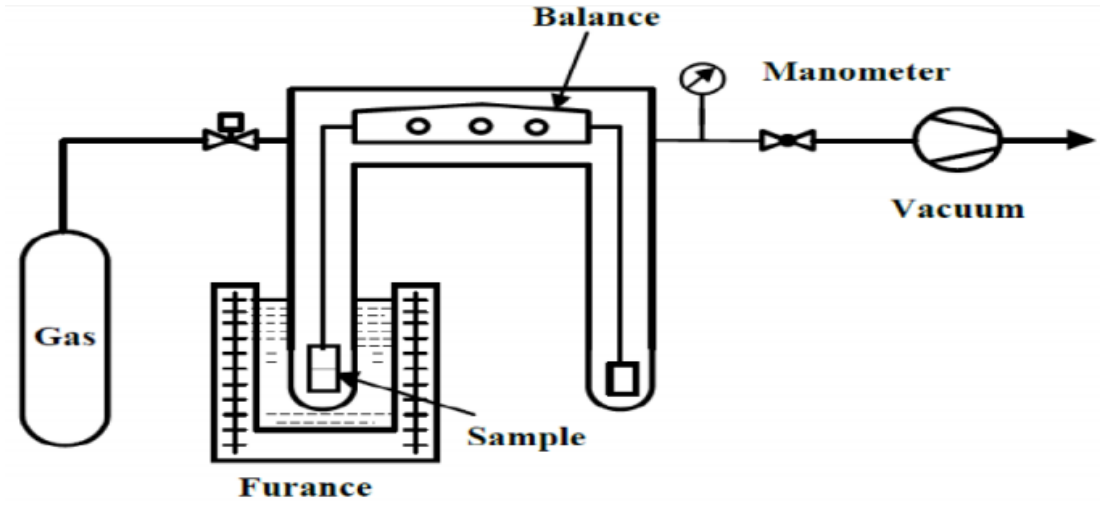

Figure 3. Gravimetric Setup for Isotherm Measurement [18]

In the gravimetric method, change in weight of the adsorbent at each specific pressure of the gas is measured. It is a direct measurement method and requires a very sensitive and accurate balance.

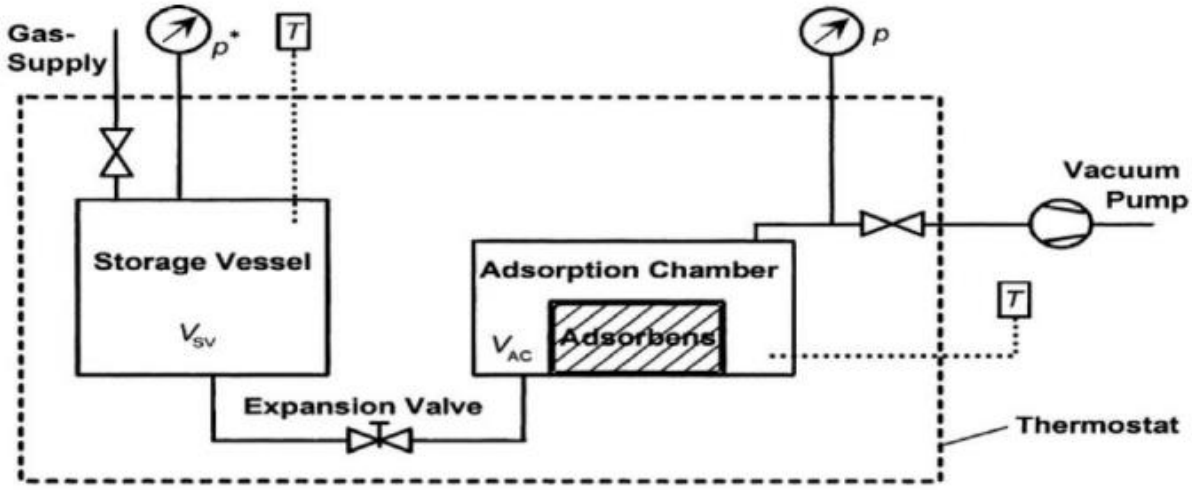

Figure 4. Volumetric Setup for Isotherm Measurement [18]

In the volumetric method, pressure change before and after expansion of the gas from the storage vessel is used to calculate the volume dosed using appropriate gas laws. After the expansion of the gas into the adsorption chamber, pressure is recorded until there is no more change in the reading which indicates an equilibrium is reached. The change in the pressure in the adsorption chamber is used to calculate the volume of gas not adsorbed. The volume adsorbed is determined from the difference of volume dosed and volume not adsorbed [15, 18].

2.2.3. Isotherm Models

To understand the equilibrium in an adsorption process, several mathematical models have been developed. Some such as those developed by Langmuir and Brunauer-Emmett-Teller (BET) are based on kinetic theories while others like the one by Freundlich is purely empirical [10, 12]. These models are based on certain assumptions and are applicable to real systems in most cases with slight modifications. Several of these relationships are briefly described in this section.

2.2.3.1.Langmuir

Type I isotherm is also called as Langmuir type isotherm because Langmuir [19] developed a model by using kinetic approach and was able to describe the type I by taking into account several assumptions. Langmuir model assumes that the adsorption occurs on a monolayer, the adsorption surface is homogeneous, and there are no lateral interactions between the adsorbed molecules [20]. This model led to a mathematical relationship for type I isotherm and is given by:

$$q = \frac{Kq_m P}{1+KP} \quad (1)$$

where q is amount adsorbed, K is the Langmuir constant, q_m is maximum amount adsorbed and P is equilibrium pressure.

2.2.3.2.Brunauer-Emmett-Teller (BET)

Brunauer-Emmet-Teller also developed a model describing adsorption equilibrium based on kinetic theory [21]. The model did not assume a monolayer adsorption as in the Langmuir model but proposed a multilayer adsorption as shown in Figure 5.

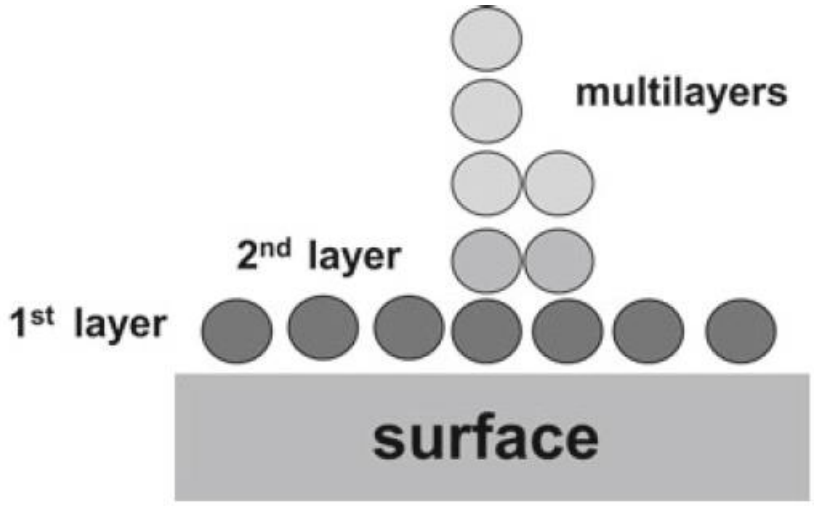

Figure 5. Schematic of Multilayer Adsorption [20]

BET model is frequently used for the characterization of porous materials and allows calculation of the surface area of porous materials. Equations 2 and 3 are used along with the experimental isotherm to determine the number of molecules required for monolayer coverage thus leading to calculation of the surface area [12].

$$Q = \frac{q_m C \frac{P}{P_o}}{\left(1-\frac{P}{P_o}\right)\left[1-\frac{P}{P_o}+C\frac{P}{P_o}\right]} \quad (2)$$

$$C = e^{\frac{E_1 - E_L}{RT}} \quad (3)$$

Q is amount adsorbed, q_m is maximum amount adsorbed, P is equilibrium pressure, P_o is saturation pressure, E_1 is heat of adsorption of first layer, E_L is heat of adsorption of second and higher layers, R is molar gas constant and T is temperature.

2.2.3.3.Freundlich

Fruendlich developed an empirical model to account for the surface heterogeneity in an adsorbent [22]. It is given by:

$$q = K_f P^{1/n} \quad (4)$$

where q is amount adsorbed, K_f is the Freunlich parameter, P is equilibrium pressure and n is heterogenity parameter.

Many adsorbents are not uniform in their distribution of the surface active sites. There could be different types of active sites some of which are easily approachable while others are not. Freunlich model includes parameters to include the extent of heterogenity in an adsorbent.

2.2.4. Isosteric Heat of Adsorption

Since adsorption is an exothermic process, heat is released when gas is adsorbed on a solid surface. This heat is known as the isosteric heat of adsorption, Qst, and is dependent on the amount of gas adsorbed due to the different types of active sites available for adsorption in an adsorbent. It also represents the strength of solid-gas interaction during the adsorption process [23, 24]. Heat of adsorption can be measured both by calorimetric and non-calometric methods [20]. In the calorimetric method, change in temperature of the adsorbent is measured with a microcalorimeter attached to the isotherm measurement setup and Qst is then calculated using the energy balance [20].

In the non-calorimetric method, natural log of pressure is plotted against the reciprocal of temperature at a constant equilibrium adsorbed amount. The slope of this linear relationship is used to determine Qst as given by equation 5 which is also known as the Clausius-Clapeyron equation [20, 25].

$$\left[\left[\frac{\partial \ln P}{\partial(\frac{1}{T})}\right]\right]_q = \frac{Q_{st}}{R} \tag{5}$$

P is pressure, T is temperature, q is uptake, Q_{st} is isosteric heat of adsorption and R is molar gas constant.

In order to use the Clausius-Clapeyron equation in determining Qst, it is important for the adsorption process being investigated to be reversible and the surface of the adsorbent should not be altered during isotherm measurements. Both calorimetric and non-calorimetric methods are reliable and comparable results have been obtained for Qst of various molecules on different adsorbents [26].

Isosteric heat of adsorption is also dependent on the surface coverage however, the extent of dependence changes with the type of adsorbent as shown in Figure 6 [24].

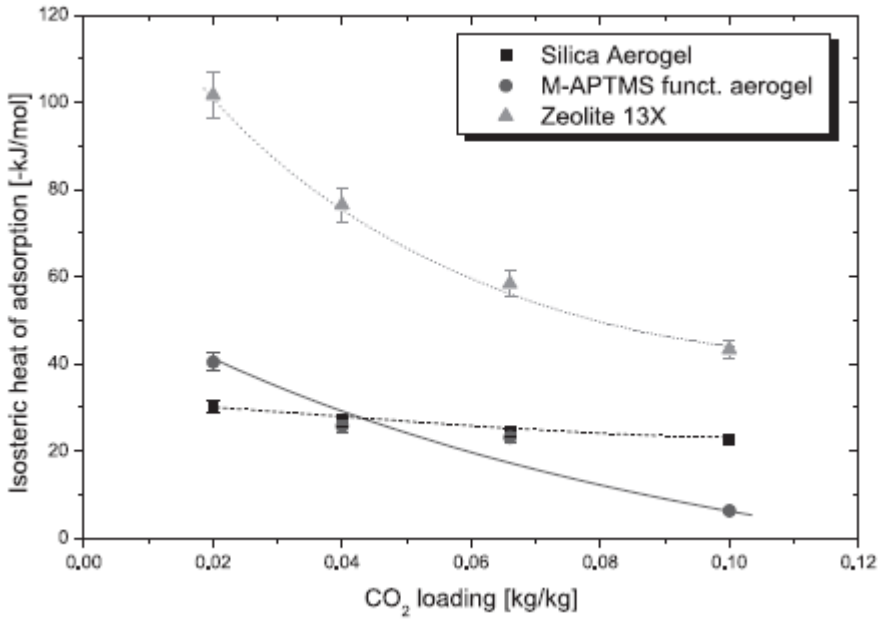

Figure 6. Dependence of Isosteric Heat of Adsorption with Loading for Different Adsorbents [24]

2.2.5. Excess and Absolute Adsorption

Adsorption amounts measured in experiments using gravimetric or volumetric methods is the Gibb's surface excess (Γ_{excess}). It is the amount of fluid that is in excess of the bulk amount that will be present in the porous material at a specific temperature and pressure [27]. For a nonporous flat surface, Gibb's surface excess is defined by:

$$\Gamma_{excess} = \int_0^{\infty} [\rho(z) - \rho_{bulk}] dz \quad (6)$$

where Γ_{excess} is the excess amount adsorbed, ρ is the density of the adsorbate, ρ_{bulk} is the density of the bulk phase and z is distance from the surface.

For porous materials, it is important to consider absolute or total adsorption for accurate modeling and designing of adsorption systems. Figure 7 outlines the difference between excess and absolute adsorption.

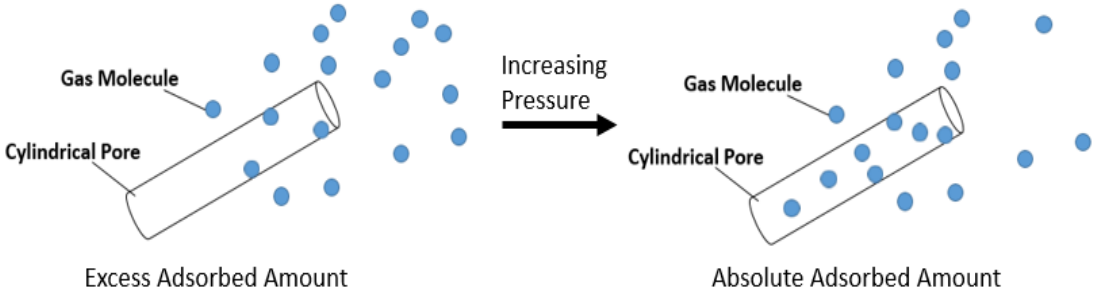

Figure 7. Excess and Absolute Adsorbed Amounts

At equilibrium, excess is the amount adsorbed on the surface of a porous material. However, when the pressure is increased, in addition to amount adsorbed on the surface, there will be bulk fluid filling up the empty space in the pores but is not adsorbed on the surface. The bulk fluid in the pores should be taken into account to determine total adsorbed amount which is given by:

$$\Gamma_{absolute} = \Gamma_{excess} + \rho_{fluid}(V_{pore} - V_{ads}) \quad (7)$$

$$V_{ads} = \frac{\Gamma_{excess}}{\rho_{ads}} \quad (8)$$

where $\Gamma_{absolute}$ is absolute adsorbed amount, Γ_{excess} is excess adsorbed amount, ρ_{fluid} is molar density of the fluid, V_{pore} is volume of the pore, V_{ads} is volume adsorbed and ρ_{ads} is density of the adsorbed phase.

Figure 8 shows the excess and absolute (total) adsorption isotherms of carbon dioxide (CO_2) on activated carbon at 318.15 K. Excess amount passes through a maximum as predicted by the Gibb's adsorption isotherm while total adsorbed amount remains constant. The maximum is also observed due to the change in density when the CO_2 changes to the supercritical phase [27].

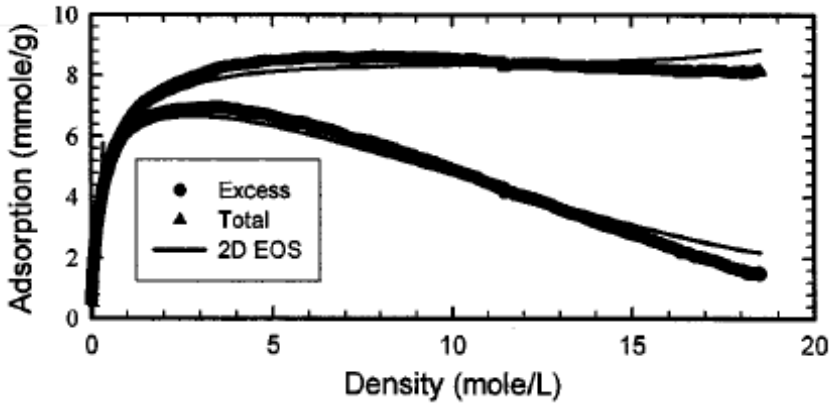

Figure 8. Adsorption Isotherms and Model for CO_2 Adsorption on Activated Carbon at 318.15 K [27]

Figure 9 shows the excess and abolute isotherms for methane (CH_4) on 13X molecular sieve at 258.15 K and 318.15 K.

At low pressures, excess and absolute adsorption could be approximately equal but at high pressures total adsorption can significantly differ from the excess adsorption in porous adsorbents depending on the pore volume [25]. It is therefore important to determine the absolute adsorption amounts when dealing with porous adsorbents.

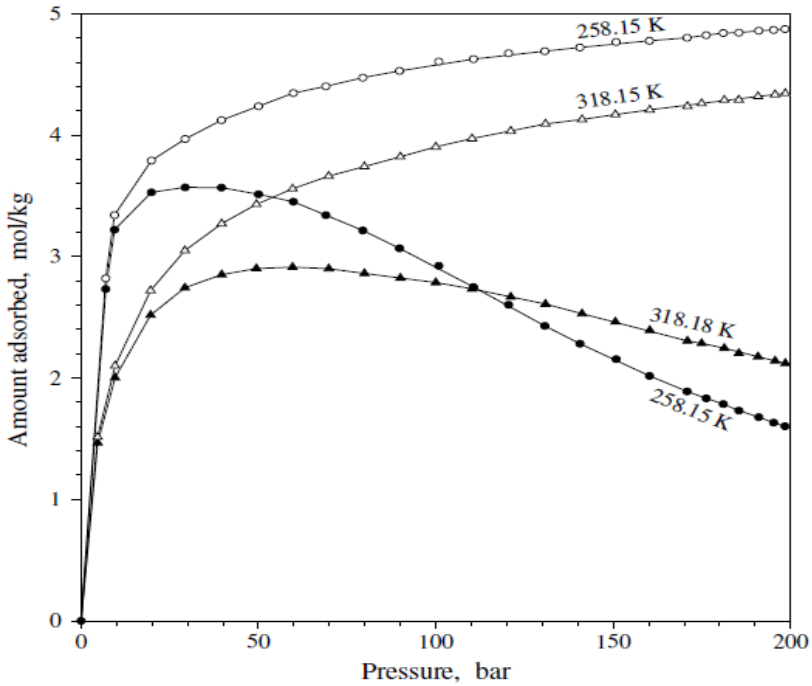

Figure 9. Adsorption Isotherms of CH_4 on 13X Molecular Sieve. Closed Symbols: Excess Adsorption. Open Symbols: Absolute adsorption [25]

2.3. Aerogels

A wide variety of materials such as activated carbon, zeolites and metal-organic frameworks (MOFs) are being used as materials for adsorption applications [28]. Aerogels, in addition to being used as materials for drug delivery and thermal insulation, may also have potential for adsorption applications especially in the field of carbon dioxide capture and storage of methane [6, 29]. Aerogels were first synthesized by Kistler in 1931 [30] and since then both inorganic and organic aerogels have beeen produced. Aerogels are highly mesoporous and are formed when the liquid in the pores of a gel is replaced by air. Their surface and pore properties are tunable and surface modification and hybridization of aerogels are also possible [5]. Silica and titania aerogels are examples of inorganic aerogels while resorcinol-formaldehyde and starch are some examples of organic aerogels. A brief overview of the synthesis procedure of various aerogels is provided in this section.

2.3.1. Silica Aerogel

Sol-gel process is used to synthesize silica aerogels. A wide variety of precursors such as tetramethoxysilane (TMOS), tetraethoxysilane (TEOS), polyethoxydisiloxane (PEDS) and methyltriethoxysilane (MTES) can be used. One way to tune the properties of an aerogel is also by using a different precursor. However, this study utilized TEOS and will refer to it in the procedure.

First, a homogenous mixture of TEOS and water is formed in the presence of ethanol to allow for better miscibility. TEOS starts to hydrolyse in the presence of water and hyroxyl groups replace the alkoxide groups in the precursor. This hydrolysis reaction is very slow, therefore, an acid catalyst such as hydrochloric acid (HCl) is added to speed up the reaction. Hydrolyzed precursor then polymerizes via a condensation reaction to

form siloxane bonds. This condensation reaction is sped up using a base catalyst such as ammonium hydroxide (NH_4OH) [31]. The reactions taking place are as follow:

$$\equiv Si - OR + H_2O \rightarrow \equiv Si - OH + R - OH$$
$$\equiv Si - OH + HO - Si \equiv \rightarrow \equiv Si - O - Si \equiv + H_2O$$
$$\equiv Si - OR + HO - Si \equiv \rightarrow \equiv Si - O - Si \equiv + R - OH \quad (9)$$

After the polymerization reaction at ambient conditions, there could be still unreacted reactants so the obtained gel is placed at 50^oC for curing in an ethanol-water solution for up to 24 hrs. This process allows complete polymerization of the reactants and formation of pores. If it is desired to have mechanically strong aerogels, silica precursor can be added to the curing solution. The presence of extra precursor allows formation of extra bonds, thereby resulting in a stronger aerogel [31].

Once the gels are cured, pore spaces are filled with ethanol, water and other impurities. To obtain aerogels, it is important to have the pores filled with a solvent that is easily miscible with a supercritical fluid. Ethanol is used frequently to wash the pores of the silica aerogel leading to alcogels. After replacing the pore fluid with pure ethanol, alcogels are dried using supercritical carbon dioixde (CO_2) because ethanol is miscible in the supercritical CO_2 and is removed from the pores keeping the structure of an aerogel intact [31]. Figure 10 shows the schematic of the silica aerogel synthesis process.

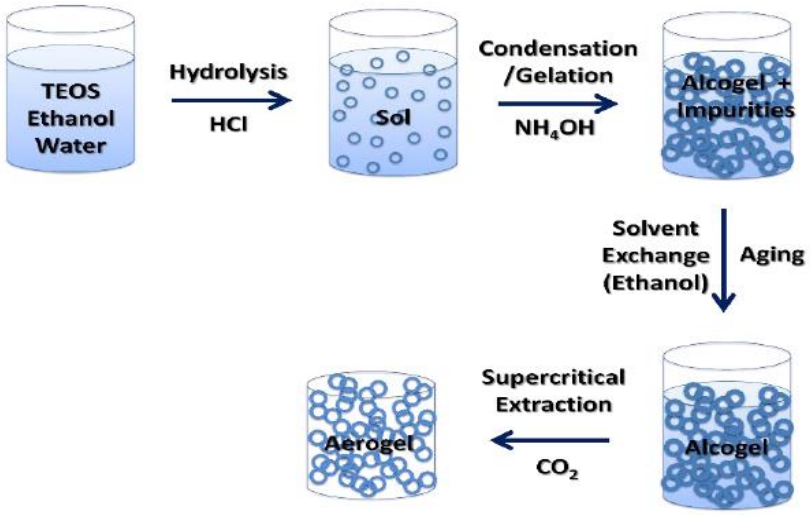

Figure 10. Schematic of Silica Aerogel Synthesis [32]

2.3.2. Resorcinol-Formaldehyde Aerogel

Pekala [33] first synthesized resorcinol-formaldehyde aerogel (RFA) in 1989 and since then it has gained significant attention in the field of thermal insulation due to its low thermal conductivity and as precursor for conductive carbon aerogel in the field of alternate energy technologies [34].

The procedure to sythesize RFA is similar to that of other aerogels. First a solution is formed by mixing resorcinol and formaldehyde in the water as a solvent. Both organic molecules starts to react together via an addition reaction. To increase the rate of the addition reaction, sodium carbonate (Na_2CO_3) is added as a catalyst which promotes deprotonation of resorcinol as shown in Figure 11 [35].

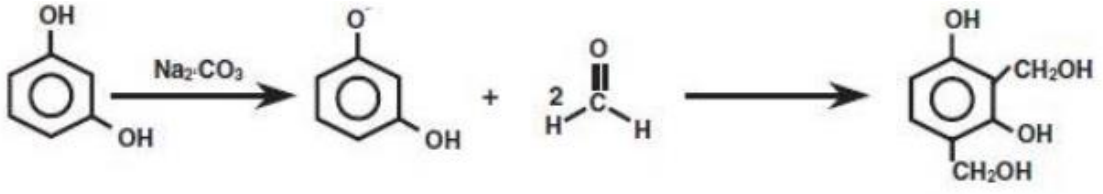

Figure 11. Catalyzed Addition Reaction of Resorcinol and Formaldehyde [35]

Deprotonation makes the medium acidic and the product of the addition reaction then polymerizes in this medium via a condensation reaction. This reaction form clusters leading to the gel whose pores are filled with water and is called hydrogel or aquagel as shown in Figure 12 [35].

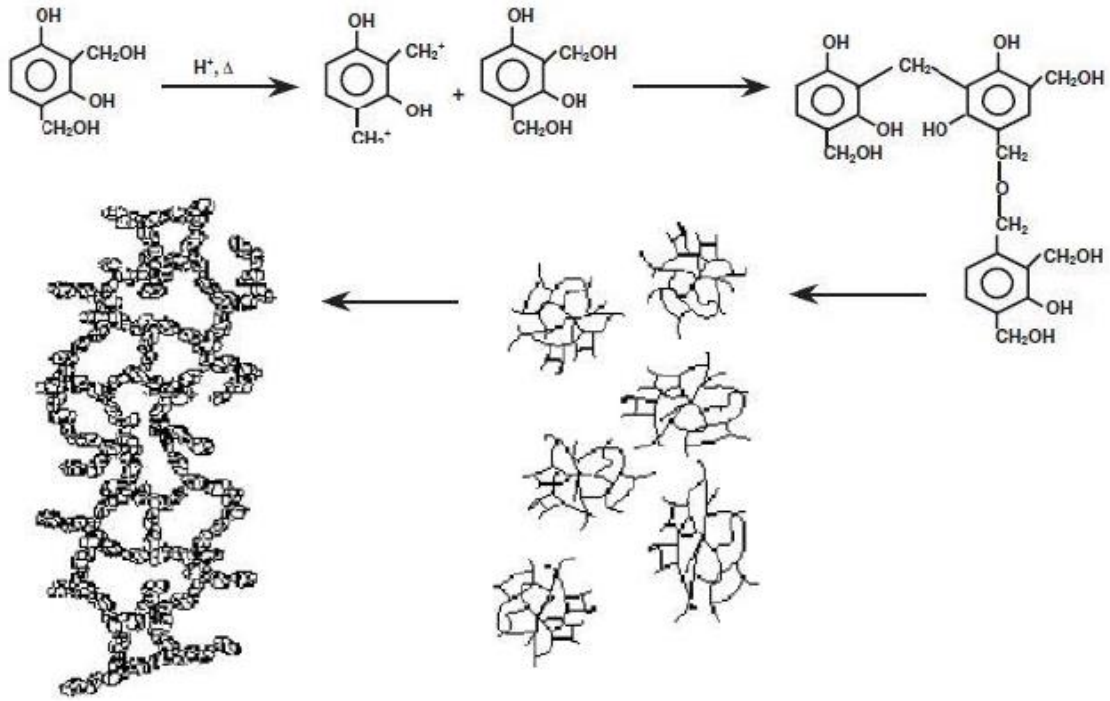

Figure 12. Gel Formation via Condensation Reaction [35]

To allow for better linkages between clusters, curing is performed at higher temperatures of 50^{o}C and 90^{o}C for around 72 hrs because curing at room temperature is very slow. Since pores are still filled with water after curing, solvent exchange is carried out to replace water with a solvent that is easily soluble in a supercritical fluid and is removed without collapsing of the pores. Acetone is commonly used as a solvent and acetogel is obtained after series of exchange steps with increasing concentration of acetone. In the end, acetogel is dried in a supercritcal extractor using carbon dioxide to remove acetone from the pores forming an aerogel. It is important to make sure that the acetogels are completely immersed in the solvent before the drying procedure. If the gels are exposed to air the interfacial tension would lead to collapse of the porous structure of

the gels and aerogels would not be obtained [35]. Figure 13 outlines the schematic of the RFA synthesis procedure.

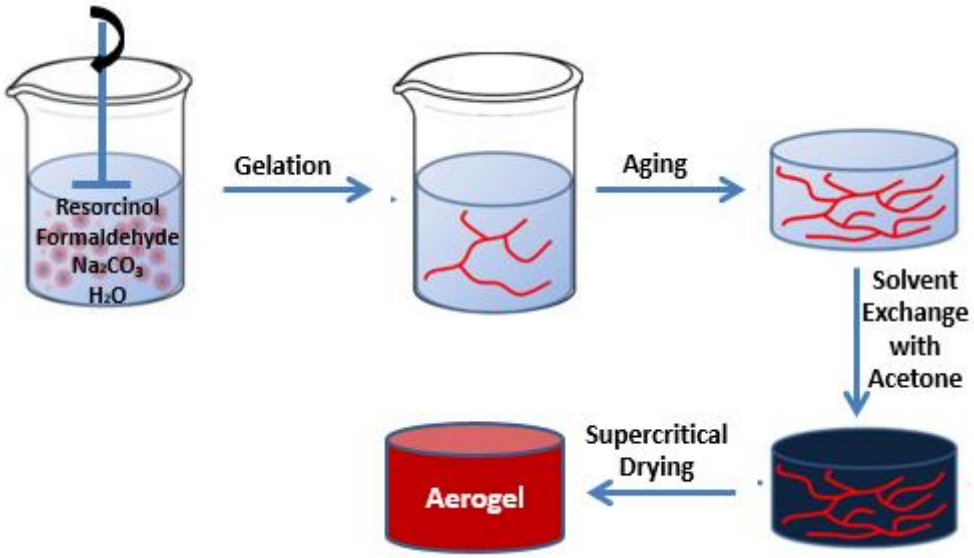

Figure 13. Schematic of Resorcinol-Formaldehyde Aerogel Synthesis

2.3.3. Carbon Aerogel

Carbon aerogels have attracted attention as interesting materials compared to other carbon based materials. It is because their properties are tunable during the synthesis procedure and they can have high surface areas and pore volumes. There are many different procedures to synthesize carbon aerogels and the most common route is the pyrolysis of the resorcinol-formaldehyde aerogel (RFA) under nitrogen (N_2) or argon (Ar) atmosphere in the temperature range of 500^{o}C – 2500^{o}C [35]. During the pyrolysis, the RFA loses functional groups containing oxygen and hydrogen and only a skeleton with pure carbon is left over. It is also possible to synthesize carbon aerogels in different monolith forms which are not only thermally stable but also stable under acidic and basic conditions [36].

2.3.4. Starch Aerogel

Starch is a polysaccharide which is found in many food sources such as wheat, potato, rice and maize. It is used as a gelling agent in a wide range of industries such as cosmetics, food and textiles. Its structure is composed of 30% amylose and 70% amylopectin polymers. These polymers produce a gel when heated at temperatures above 100^{o}C and the structure realigns when the heated gel is cooled [37]. Starch's ability to form a gel can be utilized to make starch aerogels. Starch aerogels could be advantagoeus as carriers in drug delivery systems because of their biodegradability and as adsorbents due to their porous structure [38].

Starch aerogels were first reported by Glenn and Irving in 1995 as starch microcellular foams [39] and since then different strategies have been employed to synthesize aerogels with high surface areas [38]. In this study, starch from wheat was used to synthesize the aerogel.

To synthesize starch aerogels, first a homogenous solution of starch powder in water is prepared and then the gelation takes place by heating the solution above 100^{o}C. While heating, the viscosity of the gel starts increasing and the heating is stopped when the viscosity reaches the maximum. During the gelation, inter- and intramolecular hydrogen bonds between the amylose and amylopectin polymers are broken and formed with the water. After heating, the gel is cooled to temperature of 4^{o}C for 72 hours. The cooling process is called retrogradation and the hydrogen bonds are reformed between the polymer chains during this process as shown in Figure 14 [37, 40].

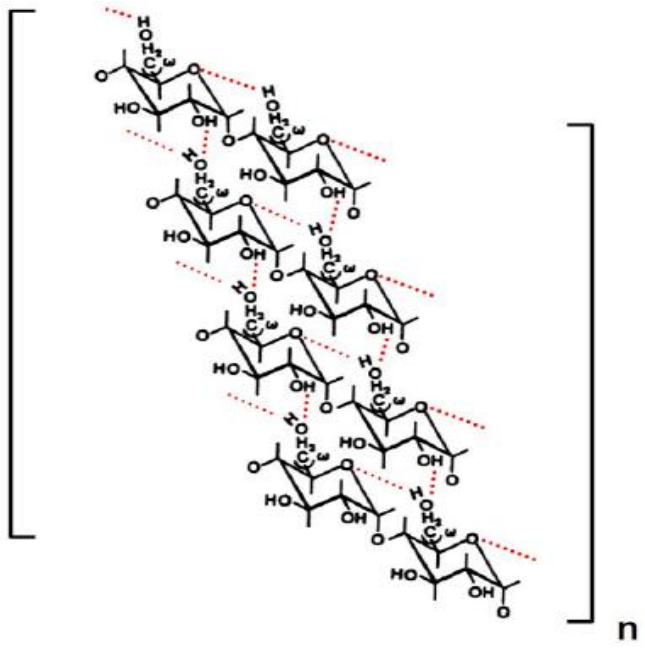

Figure 14. Hydrogen Bond Formation During Retrogradation. Dotted Red Lines: Hydrogen Bonds [37]

After retrogradation, the pores are filled with water which needs to be replaced with a solvent that is easily soluble in a supercritical fluid in order to form aerogel. Ethanol is used to replace water in the proes of the hydrogel using a series of exchange steps with increasing ethanol concentration. During this process, significant shrinkage is observed due to the loss of hydrogen bonds between water molecules and polymer chains. After solvent exchange with ethanol, alcogel is obtained which is then dried in an extractor using carbon dioxide at supercrtical conditions so that ethanol in the pores is replaced by air to form aerogel [40]. Figure 15 shows the schematic of starch aerogel synthesis procedure.

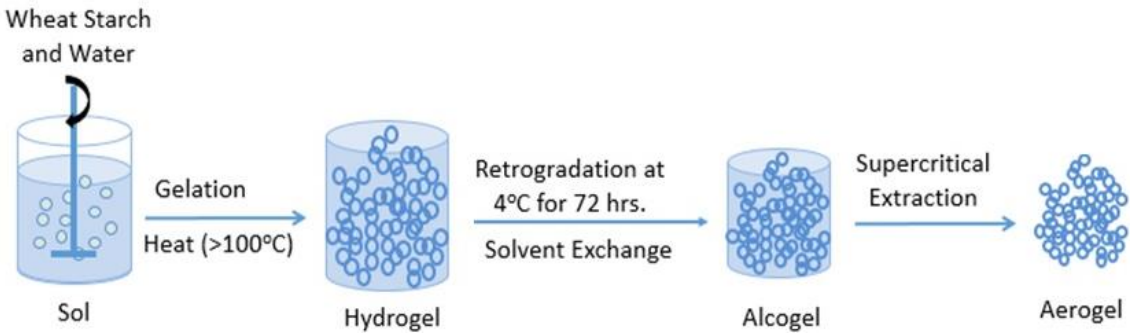

Figure 15. Schematic of Starch Aerogel Synthesis Procedure

2.4. Carbon Dioxide Adsorption

There is a need to capture the most emitted greenhouse gas, carbon dioxide, to avoid the increase of its concentration in the atmosphere which is leading to global warming and acidifying the oceans, thereby threatening natural ecosystems [41]. Different methods have been developed and are in use to capture carbon dioxide and convert it into useful chemicals or store it in the unused mines. Several of the well known methods are absorption, distillation, membrane separation and adsorption. Adsorption is being researched the most due to the low cost and low energy requirement of the technology as compared to other methods [28].

Adsorption requires the use of adsorbents and both chemical and physical adsorbents have been investigated for adsorption of carbon dioxide gas at a wide range of temperatures and pressures. Chemical adsorbents can be disadvantageous due to the difficulty in renegeration of the material, therefore, much of the work is focused on synthesizing optimum physical adsorbents and investigating them for CO_2 adsorption. For example, Siriwardane et al. [42] used activated carbon and molecular sieves to determine CO_2 adsorption capacities at 298 K and pressures up to 20 bar. Activated carbon had a maximum CO_2 adsorbed amount of 8.5 mmol/g at 20 bar while molecular sieve 13X had the adsorbed amount of 5.2 mmol/g. In another study, Cavenati et al. [43] found that molecular sieve 13X had higher adsorption amounts at high pressures and determined maximum amount to be 7.4 mmol/g at 298 K and 32 bar. In addition, Millward and Yaghi [44] used metal-organic frameworks (MOFs) for CO_2 adsorption out of which MOF-177 had the highest adsorbed amount of 35 mmol/g at 298 K and 42 bar.

A number of different native and modified aerogels have also been used for CO_2 adsorption. For some adsorption capacities were reported at a single condition of temperature and pressure while for others, adsoption isotherms were determined. Native

silica aerogel and amine impregnated silia aerogel adsorbed about 3.30 – 6.97 mmol/g of CO_2 at 298 K and 1 bar [29, 45-47] and carbon aerogels from different organic precursors adsorbed about 2.20 – 6.70 mmol/g of CO_2 at 298 K and 1 bar [48-50]. Table 1 provides a summary of most of the studies reported on aerogels for CO_2 adsorption. It is important to note that there are no studies in the literature for CO_2 adsorption on aerogels at high pressures. Also, there is no systematic study which relates the surface and pore properties of aerogels to CO_2 uptakes.

Table 1. Summary of CO_2 Adsorption Studies on Aerogels

Aerogel	**Feed Composition**	**Temperature (K)**	**Pressure (bar)**	**Maximum Capacity (mmol g^{-1})**	**Reference**
Amino-functionalized silica aerogel (5.2 wt% N)	100% CO_2	298	0.025	0.523	[5]
Amine-modified silica aerogel	10% CO_2, 10% H_2O in N_2	298	1	6.97	[29]
Amine-hybrid silica aerogel	1% CO_2 in N_2	298	1	5.55	[45]
80 wt% Tetraetylenepenta-mine loaded silica aerogel	100% CO_2	348	1	6.10	[46]
Silica aerogel	100% CO_2	298	1	3.3	[47]
Carbon aerogel (from melamine-formaldehyde resin)	100% CO_2	298	1	2.2	[48]
Carbon aerogel (from chitosan and polybenzoxazine)	100% CO_2 100% CO_2 100% CO_2	298 273 298	1 1 2	5.72 6.70 6.25	[49]
Chitosan-(20%) graphene oxide aerogel	100% CO_2	298	1	4.15	[50]

2.5. Methane Adsorption

Consumption of natural gas which consists primarily of methane (CH_4) is projected to increase by 70% in the next 20 years [1]. Large portion of consumption will be in the form of fuel because it is a cleaner fuel compared to petroleum based resources and emits 40% less greenhouse gases [4]. It has been already used as a fuel in vehicles for a long time, however the difficulty in the storage of natural gas is hindering the development of the technology. Currently it is being stored and transported in the form of compressed natural gas (CNG) and liquefied natural gas (LNG). CNG is at conditions of room temperature and pressures above 200 bar while LNG is stored at 112 K and atmospheric pressure [4]. These rigorous conditions raise concerns about the safety and cost of the natural gas as fuel. An alternative method for methane storage is in the form of an adsorbed phase in the pores or cavities of a porous material. Adsorbed natural gas (ANG) provides a safe and cost effective approach due to less rigorous working conditions [51, 52].

Adsorbents such as metal-organic frameworks (MOFs) and activated carbon are being investigated thoroughly for methane adsorption due to large surface areas of these materials. Zhou et al. [51] determined adsorption isotherms of methane on MOF5 and ZIF8 at different temperatures and pressures up to 60 bar. MOF5 adsorbed 20 wt% methane at 300 K and 60 bar while ZIF8 adsorbed around 10 wt% methane at 300 K and 60 bar. Moellmer et al. [53] measured adsorption isotherms of methane on commercially available HKUST-1 (Basolite^{TM} C300) at temperatures from 273 K – 343 K and pressures up to 500 bar. HKUST-1 had a BET surface area of 1270 m^2/g and a pore volume of 0.71 cm^3/g and had absolute adsorbed amount of 13 mmol/g at 303 K and 100 bar and 15 mmol/g at 303 K and 500 bar. In addition, Casco et al.[4] measured adsorption isotherms of methane on several different activated carbons and MOFs. Commercially available

activated carbon F400 with a BET surface area of 1070 m^2/g and pore volume of 0.55 cm^3/g had absolute adsorbed amount of 5.25 mmol/g at 298 K and 35 bar. Subsequently, laboratory synthesized activated carbon LMA738 with a BET surface area of 3290 m^2/g and a pore volume of 2.25 cm^3/g had absolute adsorbed amount of 12.63 mmol/g at 298 K and 35 bar [4].

To the best of our knowledge, studies in the literature on adsorption of methane are mostly focused on activated carbon and MOFs and there is no study of CH_4 adosrption on supercritically dried aerogels. Aerogels may also have potential as methane storage materials due to their high surface areas and pore volumes. Therefore, different inorganic and organic aerogels were investigated for CH_4 adsorption in this study and their adsorption capacities were compared with other adsorbents to evaluate their potential as adsorbents for ANG technology.

3. EXPERIMENTAL & CALCULATION METHODS

3.1. Materials

Resorcinol (99%), sodium carbonate (99.99%), and ethanol (99.9 %) were purchased from Merck. Formaldehyde (36%) was purchased from Lachema. Tetraethylorthosilicate (TEOS) (98.0 %) and ammonium hydroxide (2.0 M in ethanol) were purchased from Sigma Aldrich, and hydrochloric acid (37%) was purchased from Riedel-de Haen. Wheat Starch was purchased from Kenton (Turkey). All chemicals were used as received. Water was distilled and deionized. Carbon dioxide (99.998%), methane (99.95%), nitrogen (99.99%) and helium (99.999%) were purchased from Air Liquide.

3.2. Synthesis of Aerogels

3.2.1. Silica Aerogel

Tetraethylorthosilicate, distilled water and ethanol were mixed in the presence of acid catalyst (HCl in ethanol) for 30 min. Then base catalyst, ammonia solution in ethanol, was added and the mixture was stirred for 1 minute. The molar ratios of the chemicals, TEOS:C_2H_5OH:H_2O:HCl:NH_4OH for silica aerogel used in CO_2 adsorption measurements were 1:1.01:2.97:0.0022:0.0089. The molar ratios of the chemicals, TEOS:C_2H_5OH:H_2O:HCl:NH_4OH for silica aerogel used in CH_4 adsorption measurements were 1:0.66:0.33:0.0022:0.0089. Solution was then transferred into a mold and left for 30-40 minutes until gel was formed. Gel was then put into a solution (50% water and 50% ethanol) and placed in the oven at 50°C for 24 hours. Solvent exchange with pure ethanol was then carried out to obtain alcogel. Alcogel was dried using supercritical CO_2 for extraction of the solvent in the Applied Separations SFE unit shown in Figure 16 which consists of a high pressure extraction vessel (500 mL) in an oven given in Figure 17, a pump (A), a carbon dioxide cylinder (B), a cooler (C), a rotameter and a

control unit for controlling the temperature of the extractor and the expansion valve (D). Drying was performed at 40°C and 100 bar with a CO_2 flow rate of 1.5 L/min at STP for 8 hours. After the extraction was over, the vessel was slowly depressurized at 40°C and aerogels were obtained.

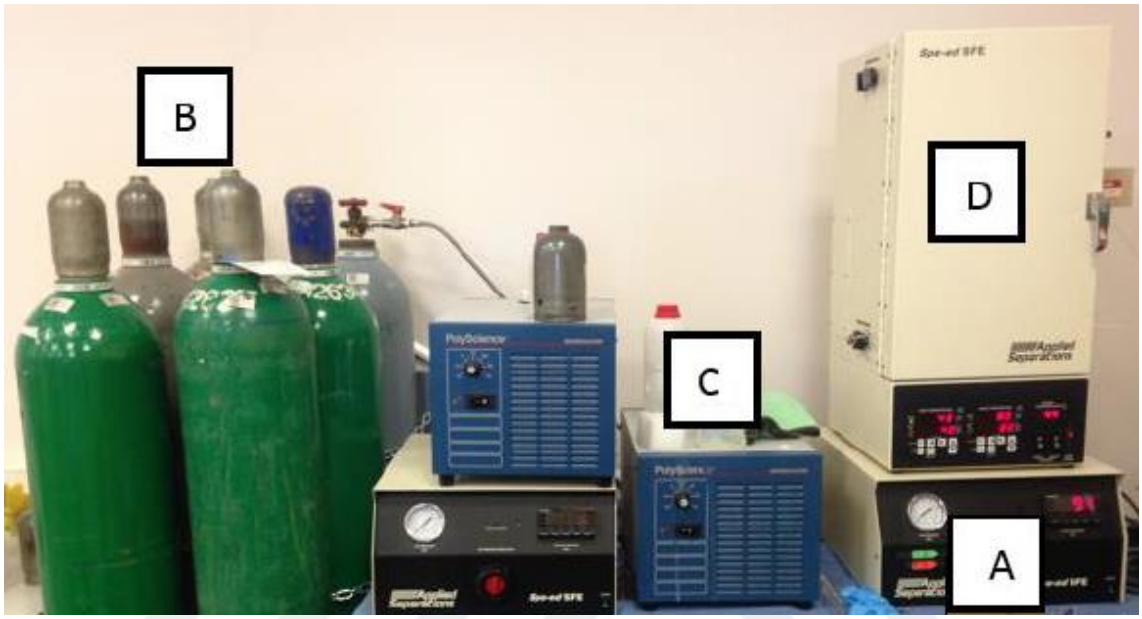

Figure 16. Supercritical Drying Unit from Applied Separations™

Figure 17. 500 mL Supercritical Extraction Vessel

3.2.2. Resorcinol-Formaldehyde Aerogel

Resorcinol-formaldehyde aerogels (RFAs) were synthesized based on the procedure described by Pekala [33]. Two different types of RFAs were synthesized based on their pore sizes. For CO_2 adsorption measurements, one had a pore size of 19 nm and another had a pore size of 7 nm. While for CH_4 adsorption measurements, one had a pore size of

17 nm and another had a pore size of 10 nm. For the preparation of RFAs, resorcinol was first dissolved in water and alkaline catalyst sodium carbonate was then added into the solution. Resulting mixture was stirred for 10 minutes and then formaldehyde was added. For the RFAs with pore sizes of 17 nm (RFA-17) and 19 nm (RFA-19), resorcinol to formaldehyde ratio of 0.5, resorcinol to alkali catalyst ratio of 50, and resorcinol to water ratio of 0.02 was used. For the RFA with pore size of 7 nm (RFA-7) and 10 nm (RFA-10), resorcinol to formaldehyde ratio of 0.5, resorcinol to alkali catalyst ratio of 200, and resorcinol to water ratio of 0.02 was used. The mixture was then poured into a sealed container. The solutions were cured at room temperature for 24 hours, for another 24 hours at 50°C, and for 72 hours at 90°C. Resulting gels were taken out of their molds and placed in acetone. Solvent exchange with pure acetone was carried out to obtain acetogels. Acetogels were dried using supercritical CO_2 for extraction of the solvent at 50°C and 138 bar with a CO_2 flow rate of 1.5 L/min for 8 hours. After the extraction was over, the vessel was slowly depressurized at 50°C and aerogels were obtained.

3.2.3. Carbon Aerogel

Carbon aerogel was prepared via pyrolysis (carbonization) of RFA-7 and RFA-10 at 1000°C in flowing N_2 (100 ml min^{-1}) for 6 hours.

3.2.4. Wheat Starch Aerogel

Wheat starch aerogel was synthesized according to the method described by De Marco et al. [40]. A homogenous starch solution with 5 wt% wheat starch was prepared in distilled water and then gelatinized at 110°C. The hydrogel was poured into molds and placed in the fridge for retrogradation at 4°C for 72 hours. Alcogel was obtained by replacing water in the pores with ethanol at room temperature. Increasing ethanol concentration (30%, 50%, 70%, 90% and two times 100% v/v) were used for solvent exchange and each exchange lasted for 24 hours. Alcogels were then dried using

supercritical CO_2 for extraction of the solvent at 40°C and 100 bar with a CO_2 flow rate of 1.5 L/min for 8 hours. After the extraction was over, the vessel was slowly depressurized at 40°C and aerogels were collected.

3.3. Surface and Pore Characterization of Aerogels

Surface and pore properties of aerogels were determined using a Micrometrics ASAP 2020® analyzer shown in Figure 18.

Figure 18. Micrometrics ASAP 2020® Analyzer

The Micrometrics ASAP 2020® instument utilizes nitrogen (N_2) adorption and desorption at a nitrogen liquid phase temperature of 77 K to measure 60-point isotherms. Brunauer-Emmet-Teller (BET) theory was employed in the instrument to calculate the surface area of aerogels while pore size distributions were derived using Barrett, Joyner and Halenda (BJH) method. In addition, saturation point was used to determine the pore volume of aerogels. Prior to analysis, samples were degassed for 5 hours under vacuum at 300°C for silica aerogel and 24 hours and 80°C for carbon, resorcinol-formaldehyde, and wheat starch aerogels.

3.4. CO_2 and CH_4 Adsorption Measurements

Excess CO_2 and CH_4 adsorption isotherms were measured using Particulate Systems' High Pressure Volumetric Analyzer (HPVA)® shown in Figure 19.

Figure 19. Particulate Systems' HPVA®

The HPVA instrument is based on a static volumetric method and uses pure helium for free space measurements. Prior to adsorption measurments, aerogel samples were degassed using the furnace A for 24 hours under vacuum at 300°C for silica aerogel and 80°C for carbon, resorcinol-formaldehyde, and wheat starch aerogels. After the degas is over, sample holder is attached to the temperature controlled analysis port B and the system is purged with helium gas using the automated valve system, the schematic of which is provided in Figure 20. After purging with helium gas, desired adsorption conditions are set and the measurement starts first by measuring free space and then adsorption measurement using CO_2 or CH_4 with an equilibration time of 10 minutes or when the pressure change is less than 0.003 bar in high pressure transducer (Pm) and 0.03 mbar in low pressure transducer (P1000).

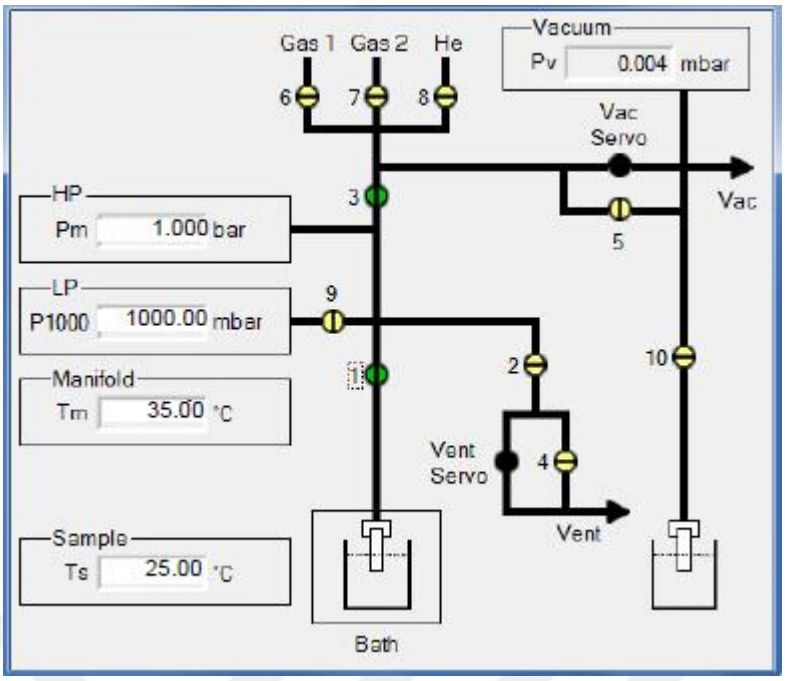

Figure 20. HPVA System Schematic

3.5. Thermodynamic Calculations

Isosteric heats of adsorption for aerogels were calculated using Clausius-Clapeyron equation 5 where the pressure and temperature relationships were obtained from isotherms at three different temperatures.

Absolute adsorption amounts were calculated from experimentally measured excess adsorption amounts by using equations 7 and 8. The molar densities of CO_2 and CH_4 at a specific temperature and pressure were obtained from NIST Chemistry Webbook [54]. Density of the adsorbed phase was assumed to be inverse of the van der Waal's constant ,b, for carbon dioxide [27, 55] while it was in the liquid density range at boiling point for methane [53].

Isotherm models were fitted to the absolute adsorption isotherms and parameters were determined using nonlinear regression in MATLAB®. The correlation coefficient, R^2, was used to evaluate the goodness of fit.

4. RESULTS & DISCUSSION

4.1. Thermodynamics of Carbon Dioxide Adsorption

4.1.1. Surface and Pore Properties of Aerogels

Surface and pore properties of aerogels used for adsorption of carbon dioxide (CO_2) were determined using nitrogen (N_2) adsorption and desorption measurements and are provided in Table 2.

Table 2. Surface and Pore Properties of Aerogels

Aerogel	**Pore Volume, V_p ($cm^3\ g^{-1}$)**	**Average Pore Diameter, D_p (nm)**	**BET Surface Area, S_{BET} ($m^2\ g^{-1}$)**	**Micropore Surface Area ($m^2\ g^{-1}$)**
Silica	4.6	15	1158	-
Resorcinol-Formaldehyde (RFA-19)	5.5	19	620	96
Resorcinol-Formaldehyde (RFA-7)	1.5	7	855	49
Carbon	3.7	16	900	342
Wheat Starch	0.57	18	128	16

Pore volumes of aerogels ranged from 0.57 cm^3/g to 5.5 cm^3/g and surface areas ranged from 128 m^2/g to 1158 m^2/g. All organic aerogels also showed certain amount of micropore surface area with carbon having the largest. Pore diameters are all in the mesoporous range and pore size distributions are given in Figure 21.

Pore size distribution curves were obtained using BJH analysis and are in the mesoporous range of 2 nm and 50 nm [13] indicating mesoporous characteristics in aerogels. Silica aerogel showed a maximum of 15 nm, RFA-19 of 15 nm, RFA-7 of 5 nm, carbon aerogel of 15 nm and wheat starch aerogel of 14.5 nm.

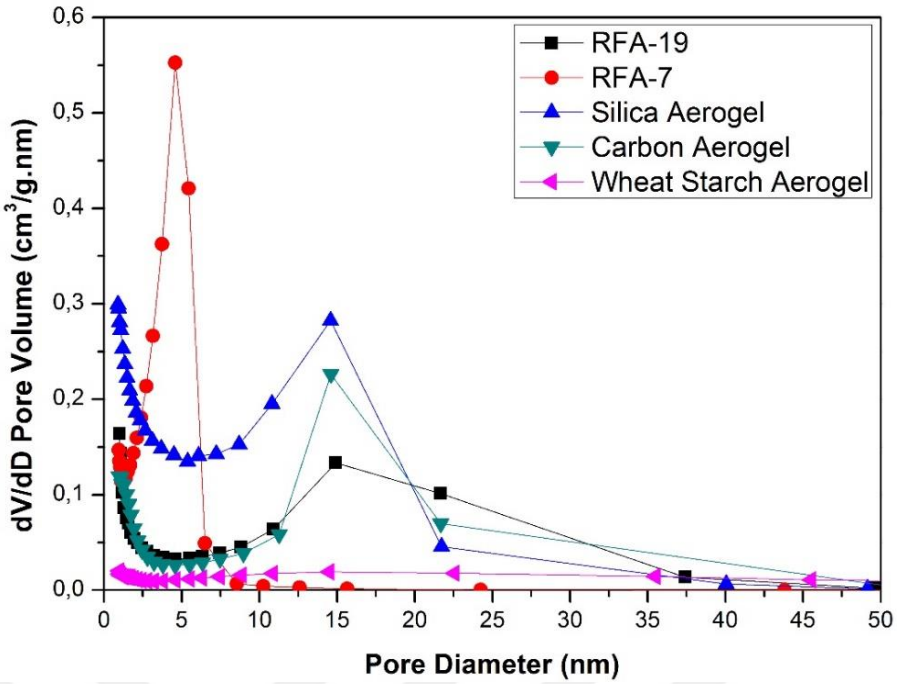

Figure 21. Pore Size Distribution of Aerogels

4.1.2. Excess Adsorption and Relationship with Surface Area

Excess CO_2 adsorption isotherms for all aerogels are shown in Figure 22 at a temperature of 308 K and pressures up to 35 bar.

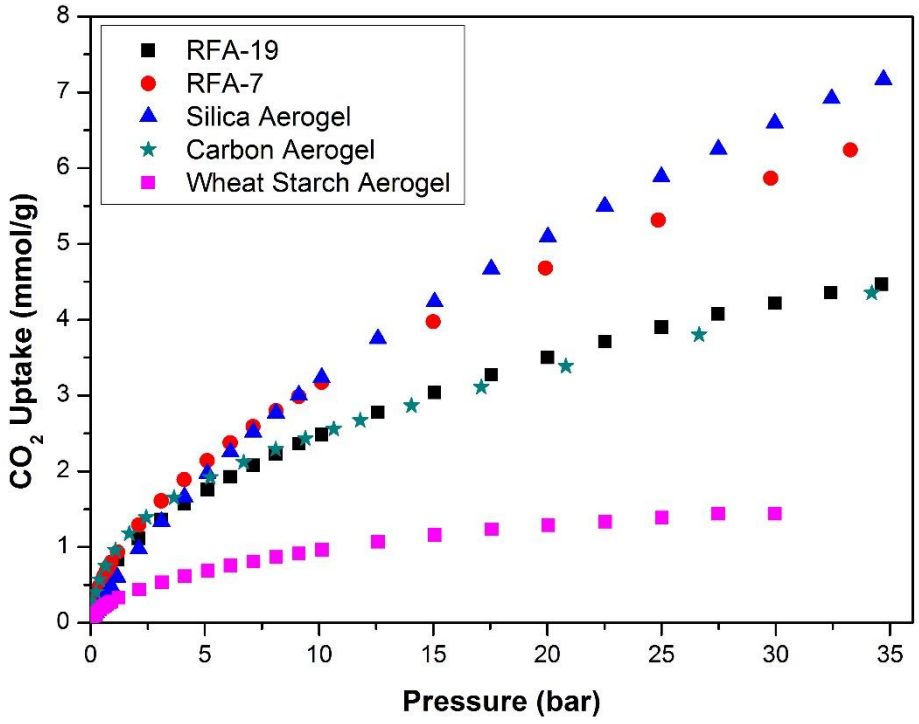

Figure 22. Excess CO_2 Adsorption Isotherms at 308 K

Silica, resorcinol-formaldehyde and carbon aerogels show increase in uptake with increase in pressure while wheat starch aerogel show increase up to a certain pressure before reaching an asymptotic value. Similar trends were also observed at 318 K and 328 K. Wheat starch aerogel had the lowest uptake due to the smallest surface area of the aerogel and silica aerogel had the highest due to the largest surface area of the aerogel.

It was also determined that the uptake at each pressure was dependent on the mesopore surface area of aerogels which was calculated from the difference of BET surface area and the micropore surface area. The relationship between the uptake and mesopore surface area at 308 K and pressures of 1 bar, 10 bar and 30 bar is shown in Figure 23.

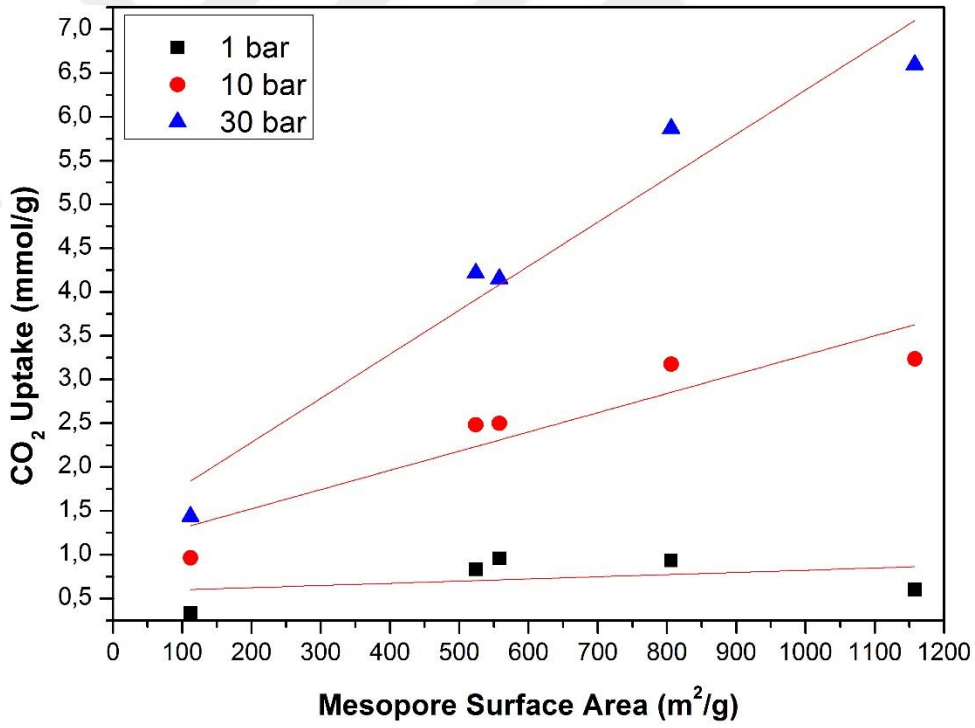

Figure 23. The Variation of Excess Uptake with Mesopore Surface Area of Aerogels at 308 K

At 1 bar, CO_2 uptake increases with surface area of aerogels except for silica aerogel which despite having the highest mesopore surface area of 1158 m^2 g^{-1} has adsorption capacity lower than that of carbon aerogel (Mesopore SA=558 m^2 g^{-1}), RFA-7 (Mesopore

SA=806 m^2 g^{-1}), and RFA-19 (Mesopore SA=524 m^2 g^{-1}). This is due to the lower affinity of CO_2 to the silica aerogel surface at low pressures [42]. At pressures of 10 bar and 30 bar, CO_2 uptake increases with mesopore surface area. This relationship is also confirmed by noting that carbon aerogel (S_{BET}=900 m^2 g^{-1}) and RFA-19 (S_{BET}=620 m^2 g^{-1}) have similar uptakes because of similar mesopore surface areas even though there is a significant difference between the BET surface area of two aerogels.

4.1.3. Excess and Absolute Adsorption Isotherms

Absolute adsorption amounts were calculated from experimentally measured excess adsorption amounts by considering the amount of bulk fluid in the pores of the aerogel and not in the adsorbed phase. Figures 24 to 28 show excess and absolute adsorption isotherms at 308 K, 318 K and 328 K for silica aerogel, RFA-19, RFA-7, carbon aerogel and wheat starch aerogel, respectively.

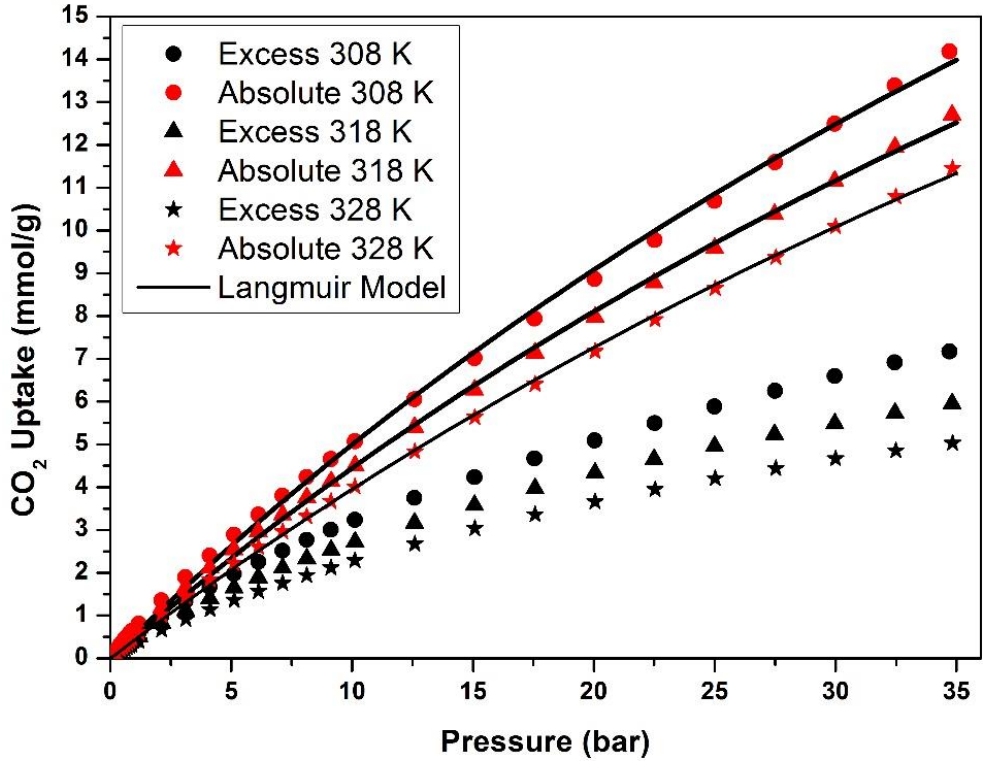

Figure 24. Excess and Absolute Adsorption Isotherms for Silica Aerogel

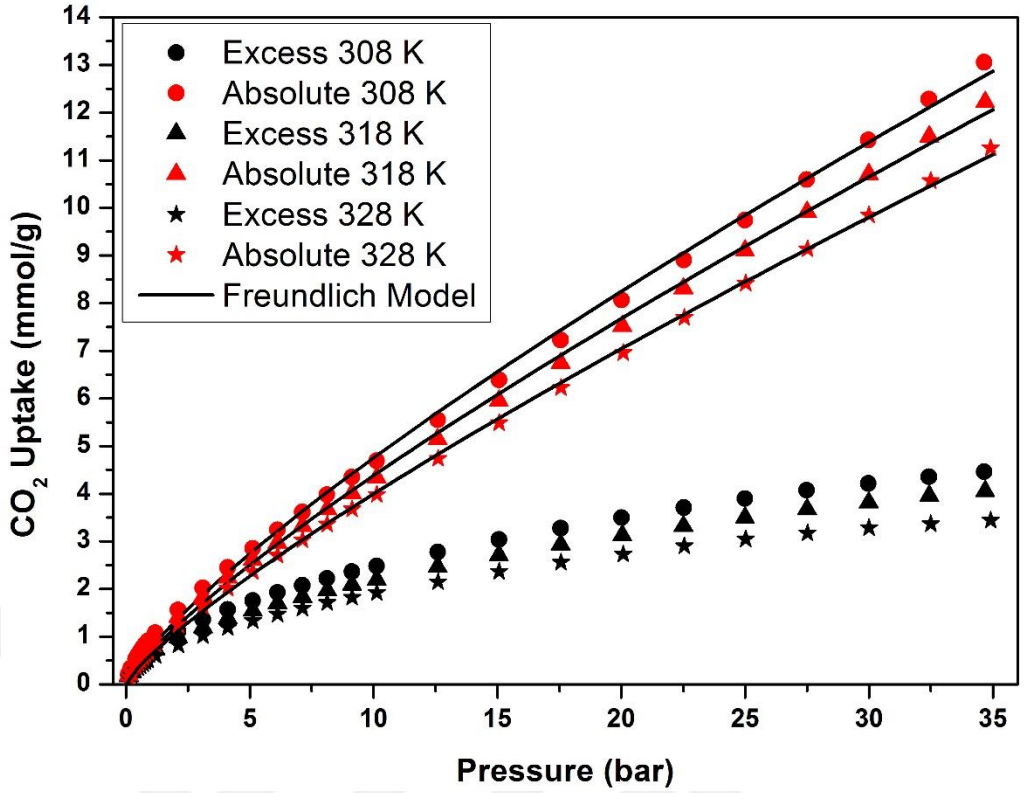

Figure 25. Excess and Absolute Adsorption Isotherms for RFA-19

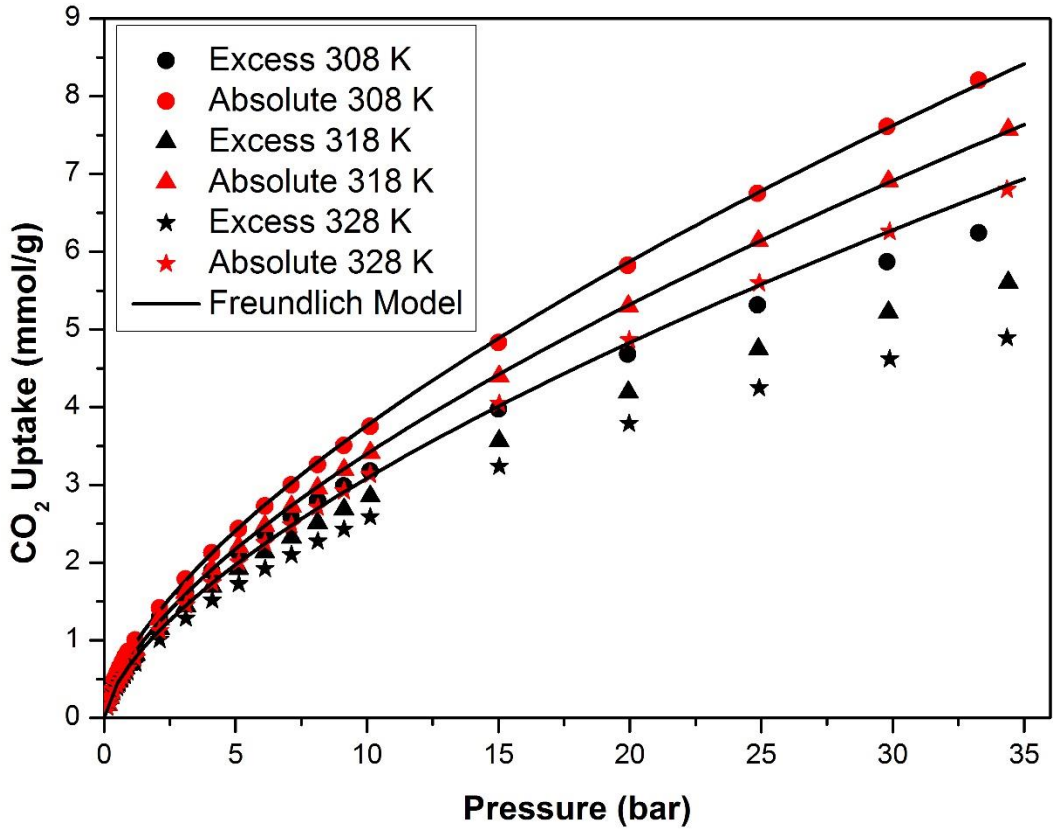

Figure 26. Excess and Absolute Adsorption Isotherms for RFA-7

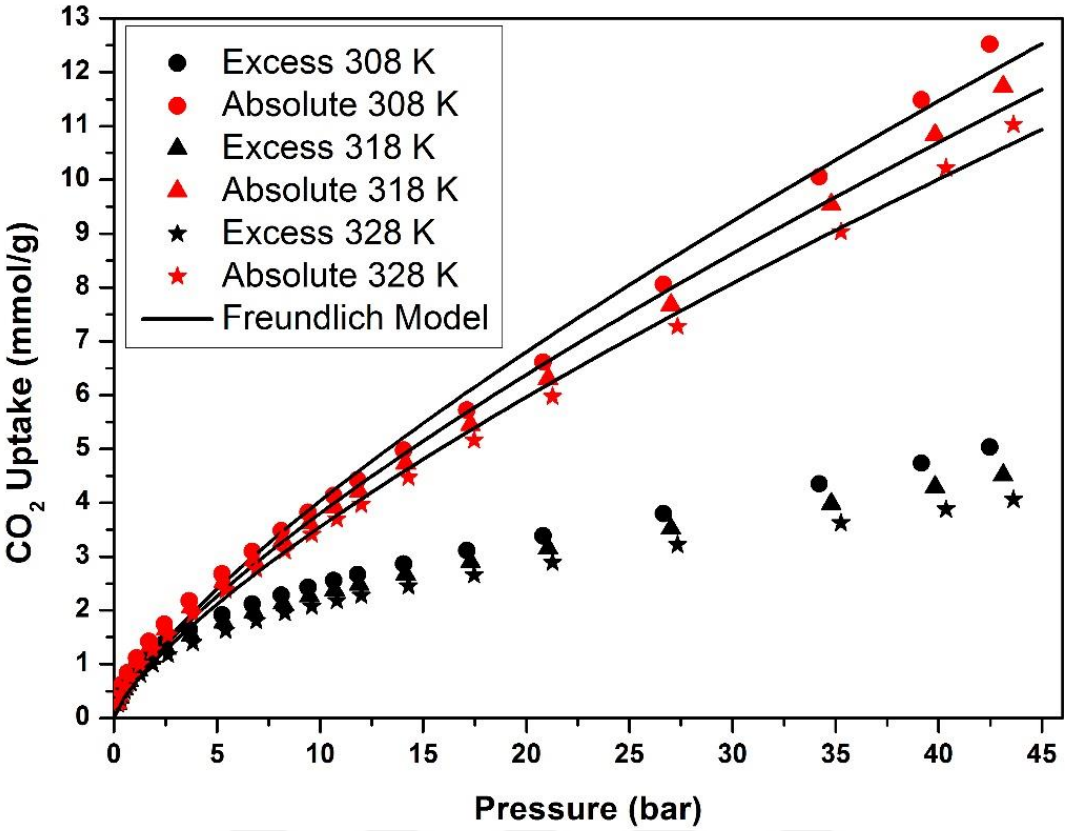

Figure 27. Excess and Absolute Adsorption Isotherms for Carbon Aerogel

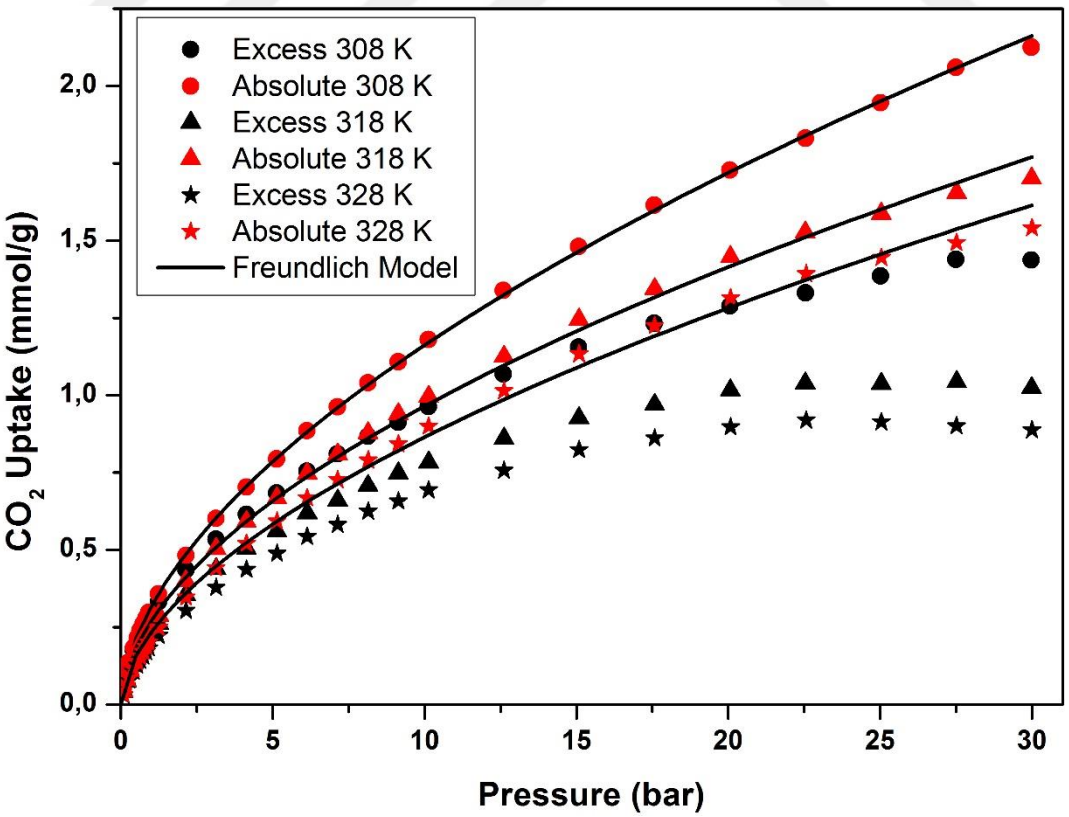

Figure 28. Excess and Absolute Adsorption Isotherms for Wheat Starch Aerogel

All isotherms are classified as type I and both absolute and excess uptake at each pressure decrease with increase in temperature for all aerogels which also indicates that the adsorption is physical and exothermic [49, 56, 57].

Since the difference between the absolute and excess adsorbed amount is dependent on the pore volume of the adsorbent, it is found that there is a significant difference between two quantities at all pressures. For silica aerogel, the difference is 34% at 1 bar and is more than 74% at pressures greater than 20 bar. Similarly, for RFA-19, the difference is 30% at 1 bar and is more than 130% at pressures greater than 20 bar. The difference for carbon aerogel is 20% at 1 bar and is more than 95% at pressures greater than 20 bar. For RFA-9, the difference is 7% at 1 bar and is more than 24% at pressures greater than 20 bar. Finally, the difference for wheat starch aerogel is 8% at 1 bar and is more than 34% at pressures greater than 20 bar. The differences among aerogels are due to the differences in pore volumes of aerogels which were given in Table 2. Silica aerogel, RFA-19 and carbon aerogel have high pore volumes which result in larger differences between total and excess adsorbed amounts. RFA-7 and wheat starch aerogel have low pore volumes which lead to smaller differences in the total and excess adsorbed amounts.

Moreover, for aerogels, excess adsorbed and absolute adsorbed amounts are not nearly equal at low pressures which is generally the case for conventional adsorbents [25]. For example, excess and absolute adsorbed amounts for activated carbon with a BET surface area of 850 m^2 g^{-1} and pore volume of 0.66 cm^3 g^{-1} were nearly equal up to pressures of almost 25 bar [27].

It would also be interesting to compare excess uptakes for carbon aerogels to other carbonaceous adsorbents. An excess adsorbed amount of about 0.008 mmol m^{-2} at 25 bar and 36°C was reported for activated carbon while carbon aerogel in this study had excess uptake of 0.004 mmol m^{-2} at 25 bar and 35°C [27]. The lower value for carbon aerogel suggests that the surface of carbon aerogel has less affinity for CO_2. However, absolute uptakes are similar due to the higher pore volume (3.7 cm^3 g^{-1}) of aerogel than activated carbon (0.66 cm^3 g^{-1}). It is, therefore, recommended that excess isotherms should be corrected at all pressures for reliable and accurate design and modeling of adsorption systems involving aerogels.

The results also indicate that some of the aerogels investigated in this study have significantly high absolute CO_2 adsorption capacities at high pressures. For instance, silica aerogel has a maximum absolute adsorption uptake of 14 mmol g^{-1} and RFA-19 has a maximum uptake of 13 mmol g^{-1} at 308 K and 35 bar, which are comparable with adsorption capacities of other adsorbents such as zeolites and activated carbon at high pressures [42, 43]. These results suggest that modified aerogels with high excess adsorption capacity at ambient conditions such as amine-modified silica aerogel prepared by Cui et al. [29] and carbon aerogel synthesized from chitosan-polybenzoxazine nanocomposites by Alhwaige et al. [49] may have really high absolute adsorption capacities at high pressures.

4.1.4. Comparsion with Other Adsorbents

In order to evaluate aerogels' potential as adsorbents for carbon dioxide capture application, it is important to compare the absolute adsorption capacities with other frequently investigated adsorbents such as activated carbon and zeolites. Figure 29 provides comparsion of CO_2 uptake of aerogels with activated carbon [27] and zeolite 13X [43] at a temperature of 308 K and 20 bar.

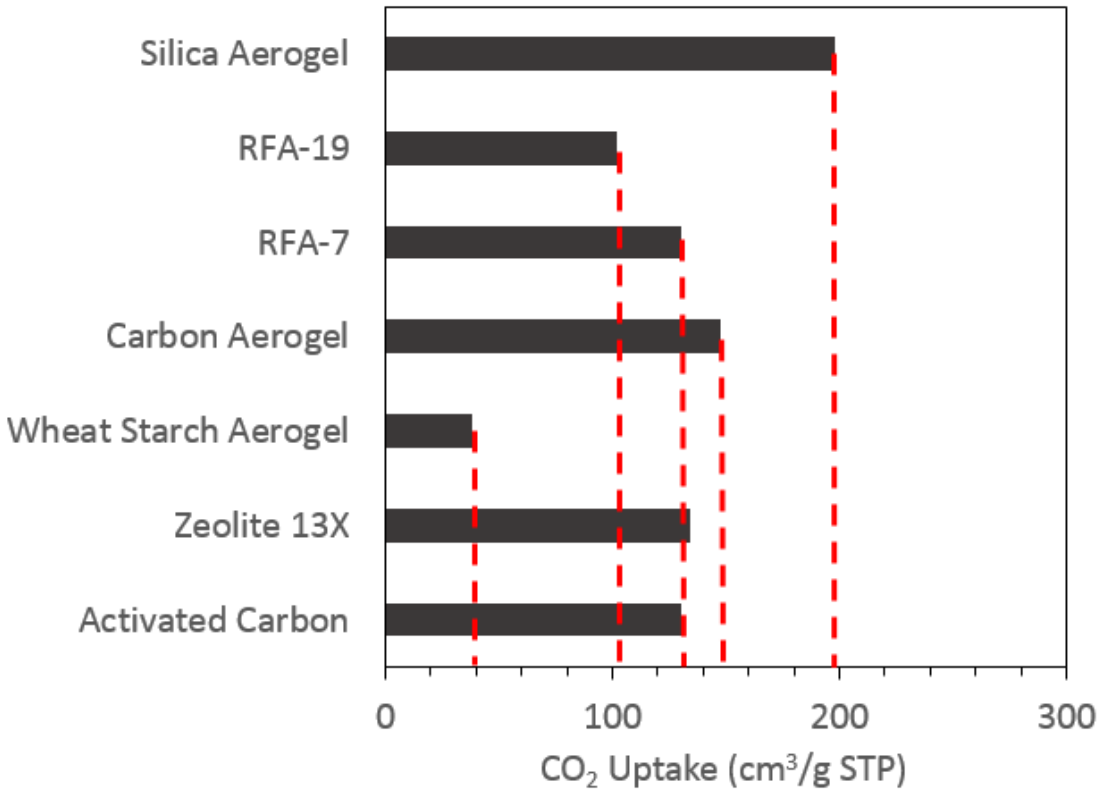

Figure 29. Comparsion of CO_2 Uptake of Aerogels with Other Adsorbents

The results indicate that at a specific temperature and pressure, aerogels have CO_2 uptakes similar and greater than zeolite 13X and activated carbon. Since properties like surface area and pore volumes are tunable for aerogels, it is possible to synthesize aerogels which would have high CO_2 uptakes. Wheat starch aerogel has the lowest uptake of all aerogels, however if a high surface area aerogel from starch with similar CO_2 uptakes to other aerogels is synthesized, it could be highly preferred over others in practical application due to the low cost and safe synthesis process.

4.1.5. Isotherm Fitting

Figures 24 to 28 also show that Langmuir isotherm model fitted the absolute adsorption data well for silica aerogel while Freundlich model fitted well for resorcinol-formaldehyde, carbon aerogel and wheat starch aerogel. This indicates that the surface of silica aerogel could be considered as homogenous. On the other hand, a good Freundlich

fit for resorcinol-formaldehyde, carbon and wheat starch aerogel reflects the heterogenity in the surface of these aerogels.

Isotherm parameters for absolute adsorption isotherms were also determined from nonlinear fitting at all temperatures and are provided in Table 3.

Table 3. Langmuir and Freundlich Parameters for All Aerogels

Temperature (K)	**308**			**318**			**328**		
Freundlich Parameters	K_f	n	R^2	K_f	n	R^2	K_f	n	R^2
Carbon Aerogel	0.7134	1.329	0.9946	0.6832	1.341	0.9959	0.6356	1.338	0.9969
RFA-19	0.7622	1.258	0.9985	0.6812	1.237	0.9988	0.6104	1.225	0.9994
RFA-7	0.8568	1.556	0.9998	0.7681	1.548	0.9999	0.6957	1.546	0.9999
Wheat Starch Aerogel	0.3165	1.77	0.9997	0.2706	1.811	0.9980	0.2338	1.76	0.9968
Langmuir Parameters	K (bar^{-1})	q_m (mmol g^{-1})	R^2	K (bar^{-1})	q_m (mmol g^{-1})	R^2	K (bar^{-1})	q_m (mmol g^{-1})	R^2
Silica Aerogel	0.01110	49.98	0.9988	0.01076	45.77	0.9992	0.009622	45.01	0.9995

4.1.6. Isosteric Heat of Adsorption

Excess adsorption isotherms measured at temperatures of 308 K, 318 K and 328 K for all aerogels were used to determine isosteric heat of adsorption ,Qst. It is an important thermodynamic quantity because it can provide information on whether the adsorption is physical or chemical as well on the strength of adsorbate-adsorbent interactions [23]. According to the Clausius-Clapeyron equation 5, plots of lnP against 1/T at a constant uptake were created for all aerogels and are shown in Figures 30-34.

The slopes of the lnP versus 1/T plots were used to calculate Qst at different uptakes and the dependence on uptake is provided in Figure 35.

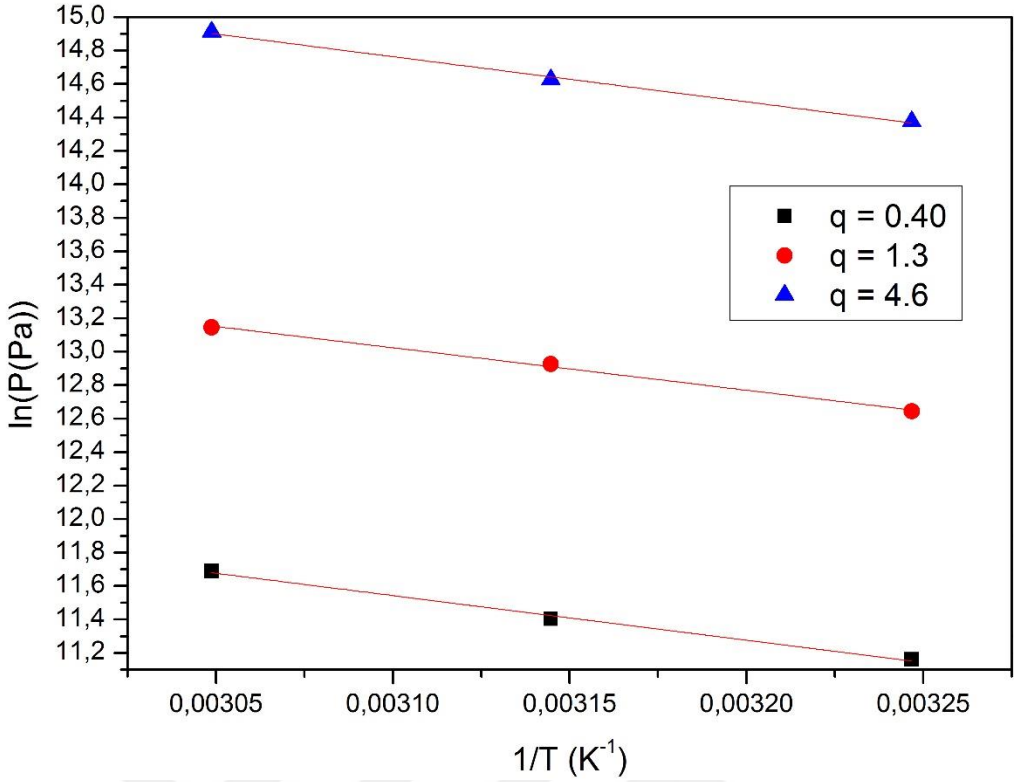

Figure 30. Relationship between lnP and 1/T for Silica Aerogel

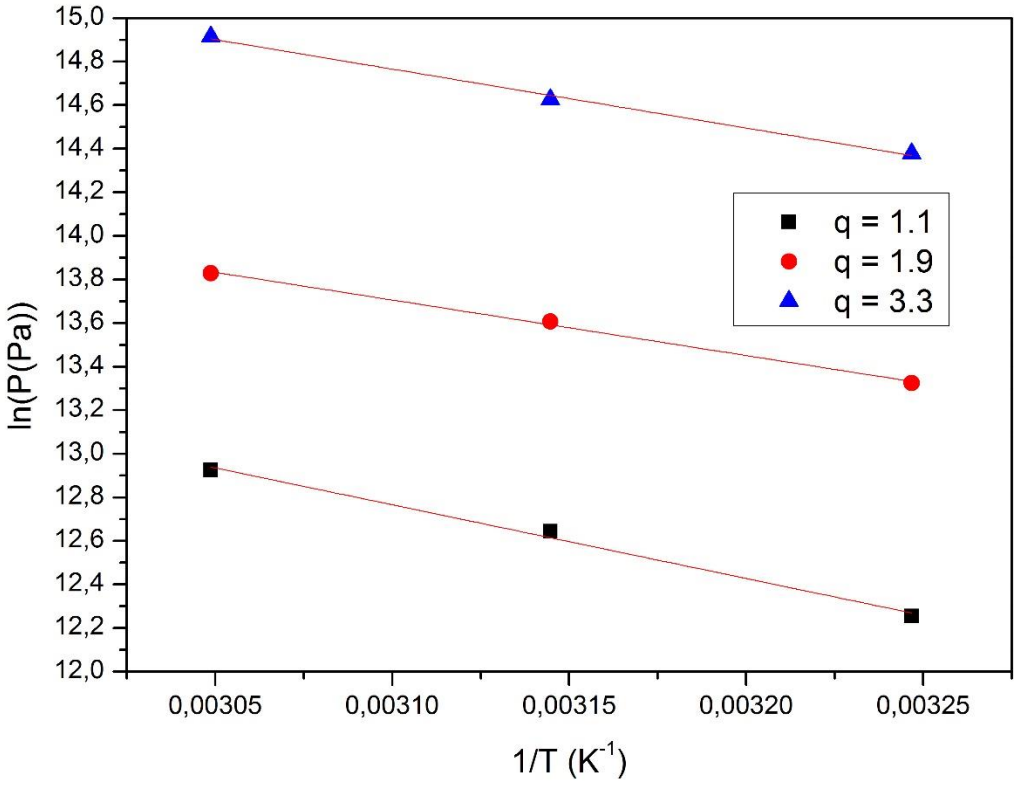

Figure 31. Relationship between lnP and 1/T for RFA-19

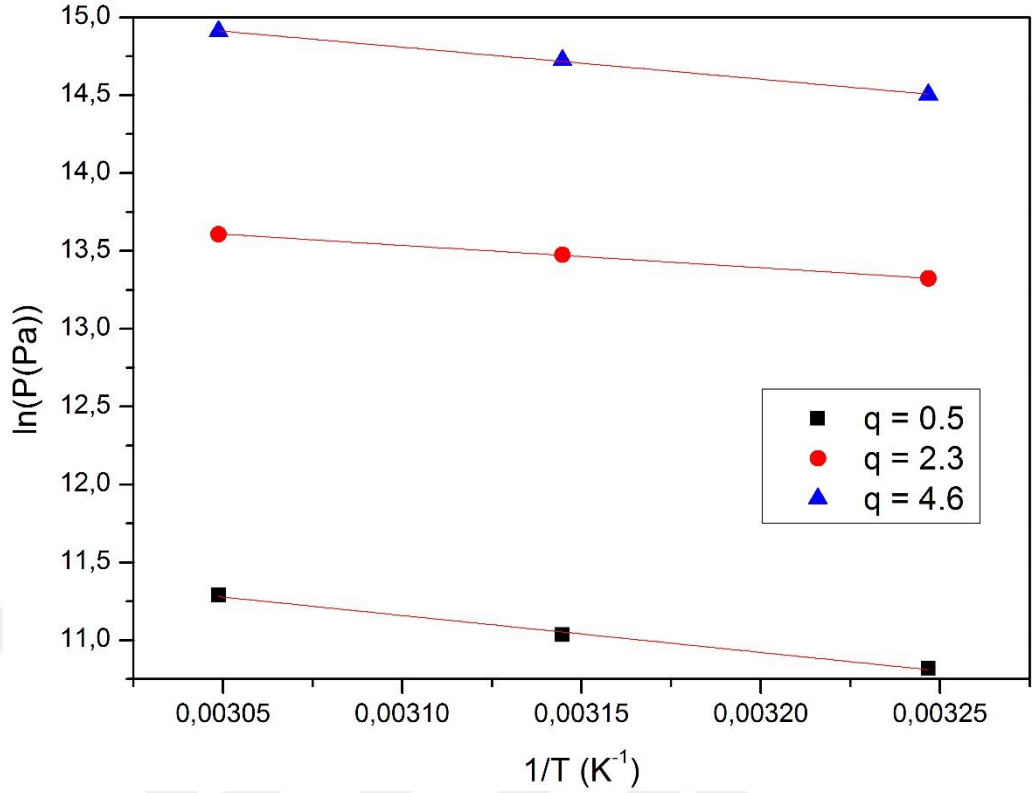

Figure 32. Relationship between lnP and 1/T for RFA-7

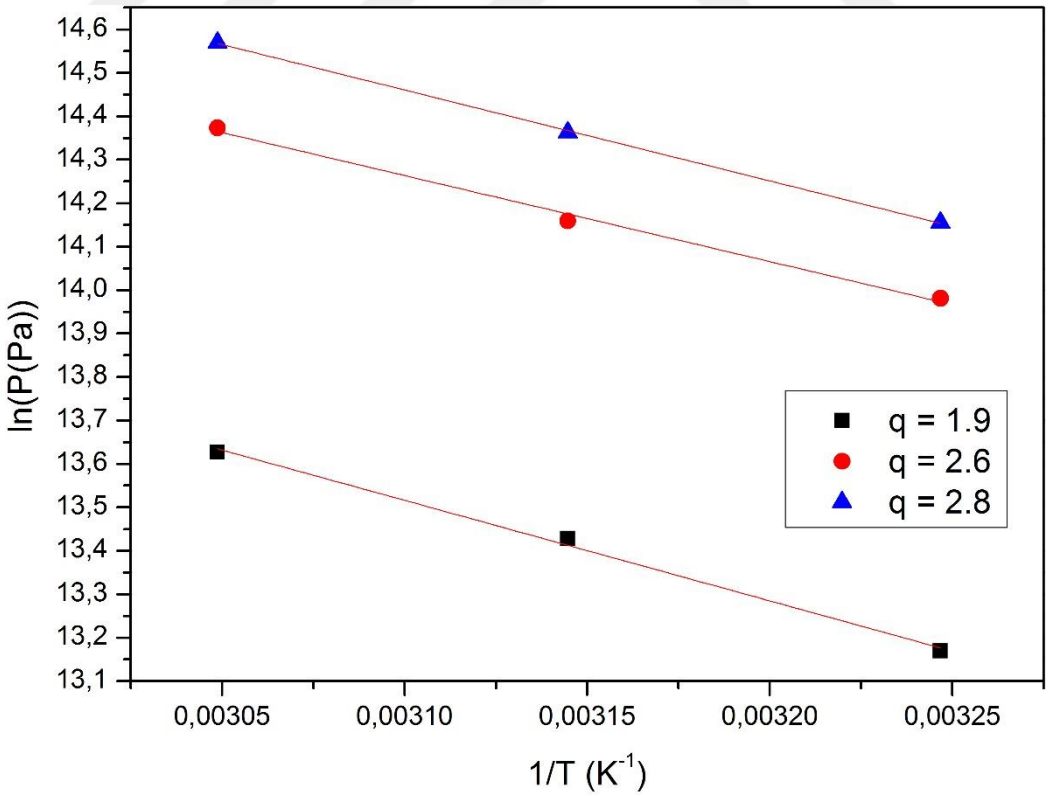

Figure 33. Relationship between lnP and 1/T for Carbon Aerogel

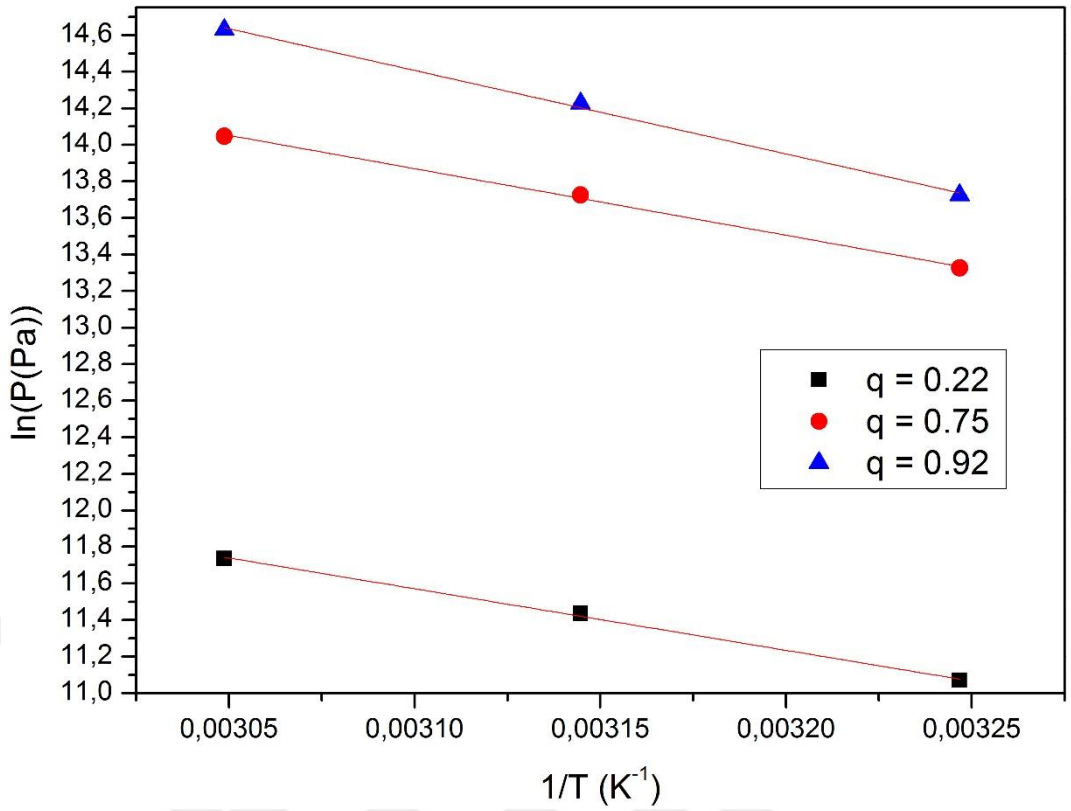

Figure 34. Relationship between lnP and 1/T for Wheat Starch Aerogel

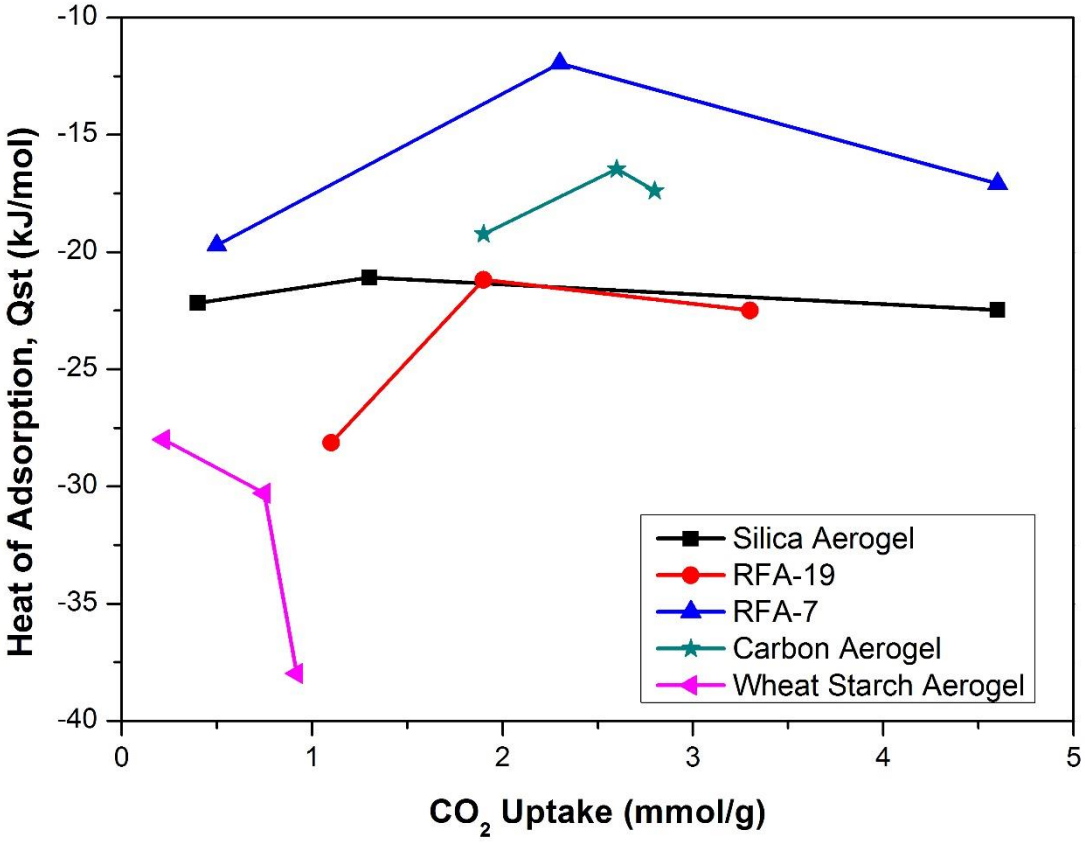

Figure 35. Variation of Heat of Adsorption with CO_2 Uptake for Different Aerogels

It can be seen from Figure 35 that Qst values are dependent on the uptake for organic aerogels but is approximately constant for silica aerogel. It is common for silica aerogel to depict independency between heat of adsorption and uptake due to its homogenous surface [24] allowing similar interactions at all active sites. All Qst values are negative and less than 50 kJ/mol. Negative values confirms the exothermicity of the adsorption process and smaller values show that the adsorption is physical. The higher the value of Qst, the stronger is the interaction of CO_2 with the aerogel. The highest values for wheat starch aerogel among all the aerogels investigated in this study indicate the strongest interaction of CO_2 molecules with surface active sites, however, the uptake is low due to low surface area of the aerogel. The lowest values for RFA-7 are indicative of weak interaction of CO_2 with surface active sites.

The average value for carbon aerogel is approximately -17.7 kJ/mol which is comparable with the value of -19.23 kJ mol^{-1} reported for activated carbon [58] and the value of -17.2 kJ mol^{-1} reported for the carbon aerogel synthesized from chitosan-polybenzoxazine nanocomposite [49]. The average heat of adsorption of silica aerogel is -21.9 kJ/mol which is similar to the value of -22 kJ mol^{-1} reported for mesoporous silica, MCM-41 [59]. Heat of adsorption of CO_2 on resocinol-formaldehyde and wheat starch aerogels are reported for the first time in this study. In addition to determining the type of adsorption process from the low values of Qst, these values also reflect the low energy requirement for the regeneration of adsorbents which is crucial in the designing of adsorption processes for CO_2 capture.

4.2. Thermodynamics of Methane Adsorption

4.2.1. Surface and Pore Properties of Aerogels

Surface and pore properties of aerogels used for investigation of adsorption of methane (CH_4) were determined using nitrogen (N_2) adsorption and desorption measurements and are provided in Table 4.

Table 4. Surface and Pore Properties of Aerogels

Aerogel	Pore Volume, V_p ($cm^3\ g^{-1}$)	Average Pore Diameter, D_p (nm)	BET Surface Area, S_{BET} ($m^2\ g^{-1}$)	Micropore Surface Area ($m^2\ g^{-1}$)
Silica	2.70	12	906	-
Resorcinol-Formaldehyde (RFA-17)	3.95	17	925	79
Resorcinol-Formaldehyde (RFA-10)	1.46	10	604	79
Carbon	3.30	24	549	163

Pore volumes of aerogels ranged from 1.46 cm^3/g to 3.95 cm^3/g and surface areas ranged from 549 m^2/g to 925 m^2/g. Resorcinol formaldehyde and carbon aerogels also had certain amount of micropore surface area with carbon having the largest. Pore diameters are all in the mesoporous range and pore size distributions are given in Figure 36.

Pore size distribution curves were obtained using BJH analysis and are in the mesoporous range of 2 nm and 50 nm [13] indicating mesoporous characteristics in aerogels. Silica aerogel show a maximum of 14 nm, RFA-17 of 12 nm, RFA-10 of 35 nm and carbon aerogel of 14 nm.

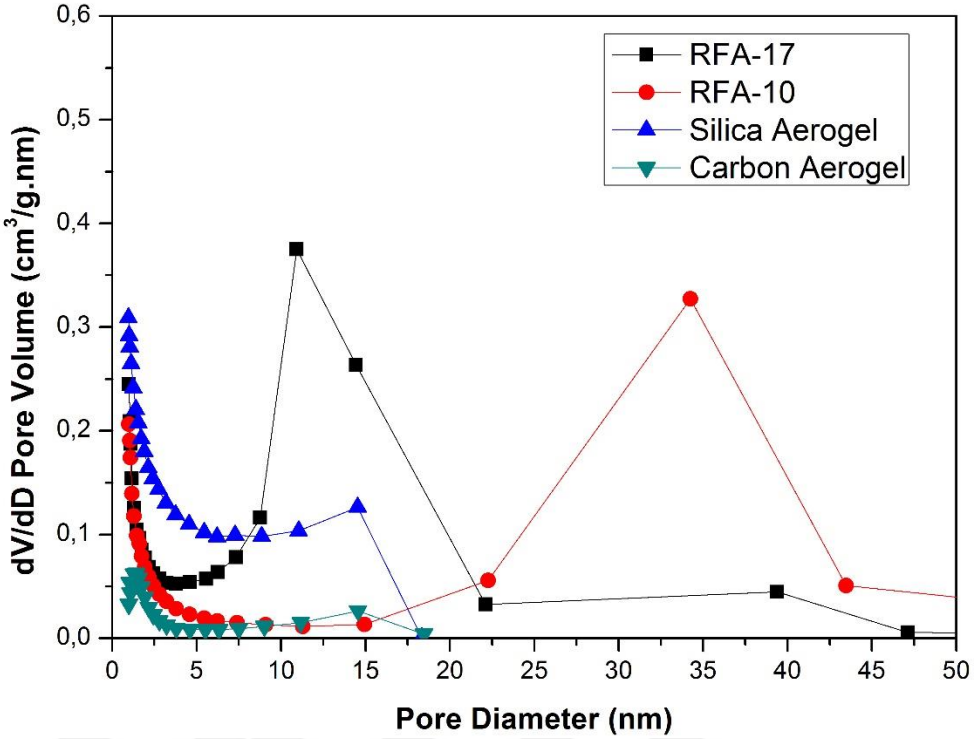

Figure 36. Pore Size Distribution of Aerogels

4.2.2. Excess Adsorption and Desorption

Excess CH_4 adsorption isotherms for all aerogels are shown in Figure 37 at a temperature of 298 K and pressures up to 100 bar.

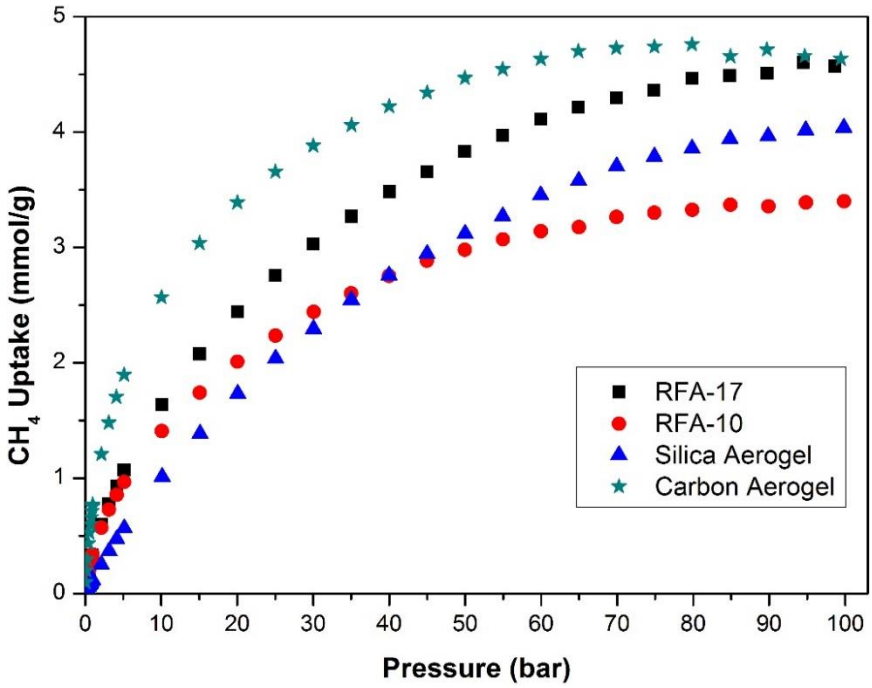

Figure 37. Excess CH_4 Adsorption Isotherms at 298 K

It is noted from Figure 37 that CH_4 uptake increases with pressure for all aerogels before reaching a maximum value. The Gibbs excess adsorption phenomenon in which uptake increases up to a maximum and then decreases with increasing pressure can be observed for carbon aerogel [60]. The pressures are not sufficiently high for this phenomenon to be observable in other aerogels.

In addition, it is also interesting to note that carbon aerogel with the lowest BET surface area had the highest uptake of all aerogels followed by RFA-17, RFA-10 and silica aerogel. Comparing silica aerogel and RFA-10, uptake is higher for RFA-10 up to 35 bar and lower at pressures greater than 40 bar. Similar trends were also observed at temperatures of 308 K and 318 K. These differences in uptakes and independency on the BET surface area can be described by the effect of micropore surface area on the adsorption of methane. Since the methane is at supercritical conditions, it is well known that methane adsorption occurs via filling of micropores and has been proven via various correlations [61]. Adsorption of methane in micropores can be explained by comparing carbon aerogel and RFA-17. Even though RFA-17 has a much higher BET surface area, CH_4 uptake is lower than carbon aerogel up to 90 bar due to lower micropore surface area. The difference in behavior of adsorption between silica and RFA-10 can also be related to micropore adsorption. Since silica aerogel does not have any micropores, the uptake is lower than that of RFA-10 at low pressures, however after filling of micropores, uptakes are higher for silica aerogel due to the high BET surface area.

In order to be able to use aerogels as adsorbents for storing methane in vehicles, it is important that the adsorbed amount of methane is useable and the adsorbent is easily regenerated. Figures 38-41 show excess adsorption and desorption isotherms of methane for all aerogels at temperatures of 298 K, 308 K and 318 K and pressures up to 120 bar.

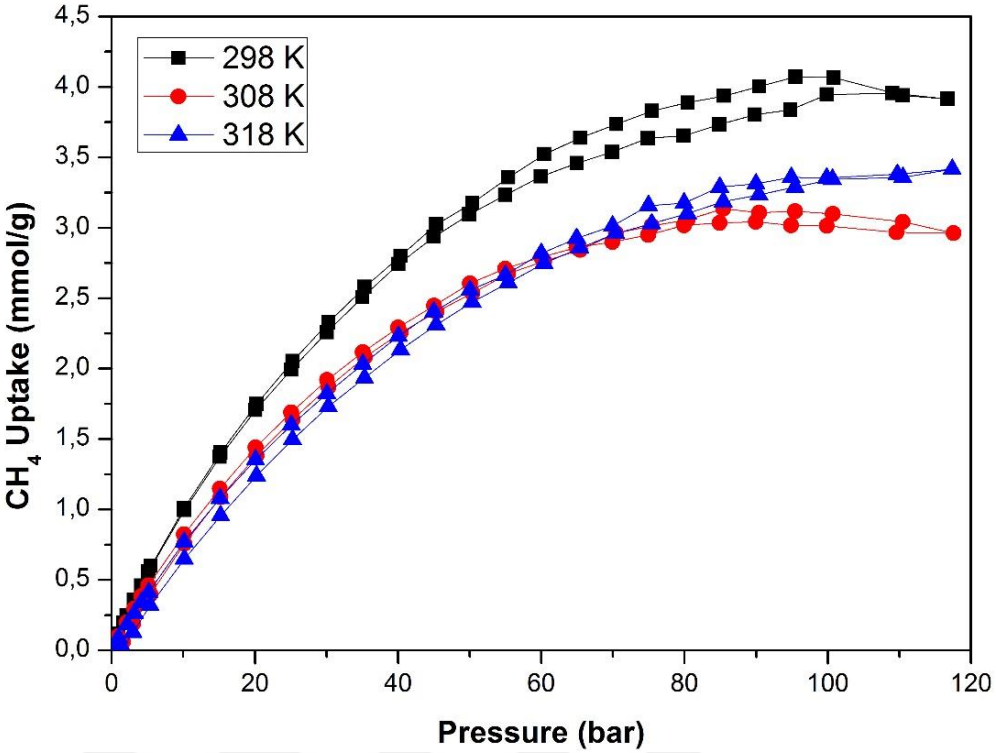

Figure 38. Excess CH_4 Adsorption and Desorption Isotherms for Silica Aerogel

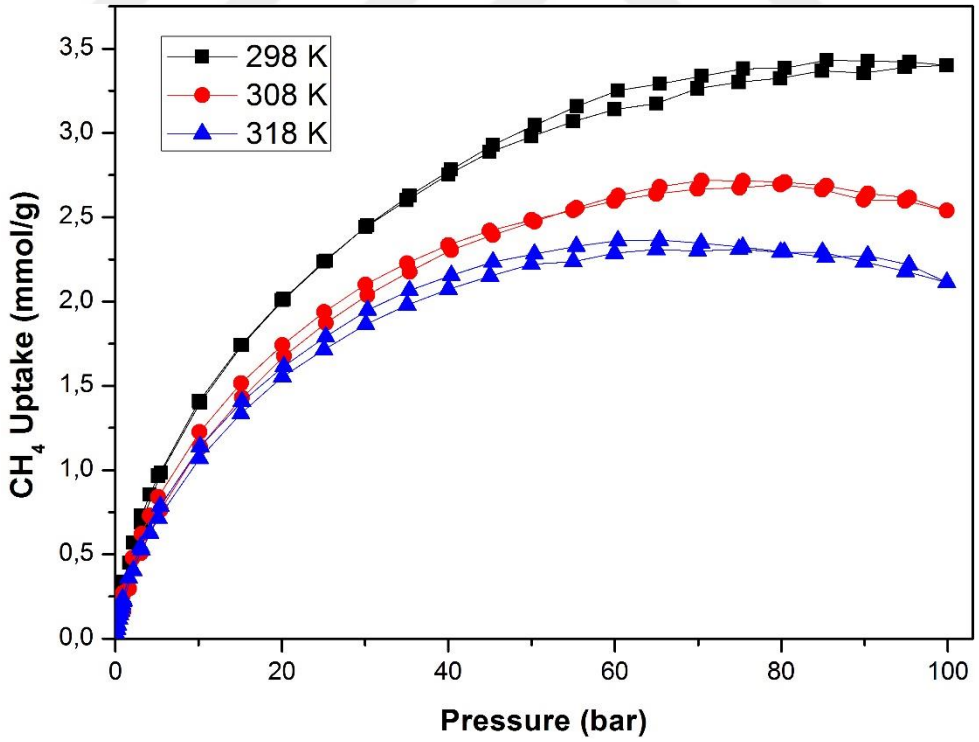

Figure 39. Excess CH_4 Adsorption and Desorption Isotherms for RFA-10

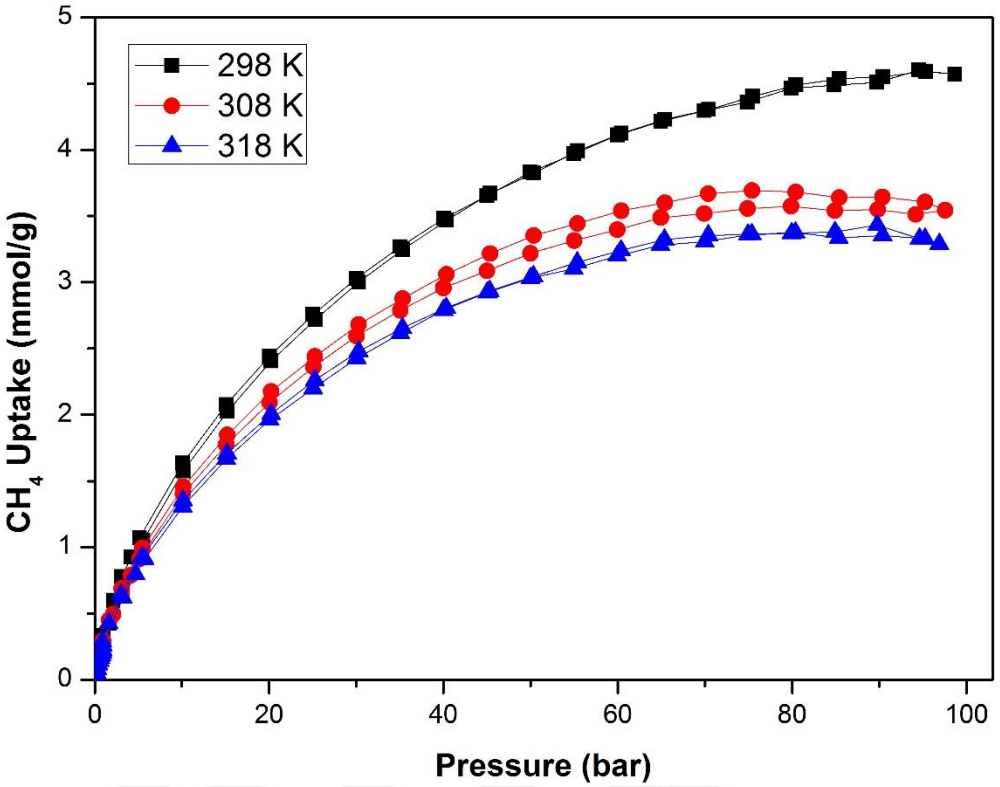

Figure 40. Excess CH_4 Adsorption and Desorption Isotherms for RFA-17

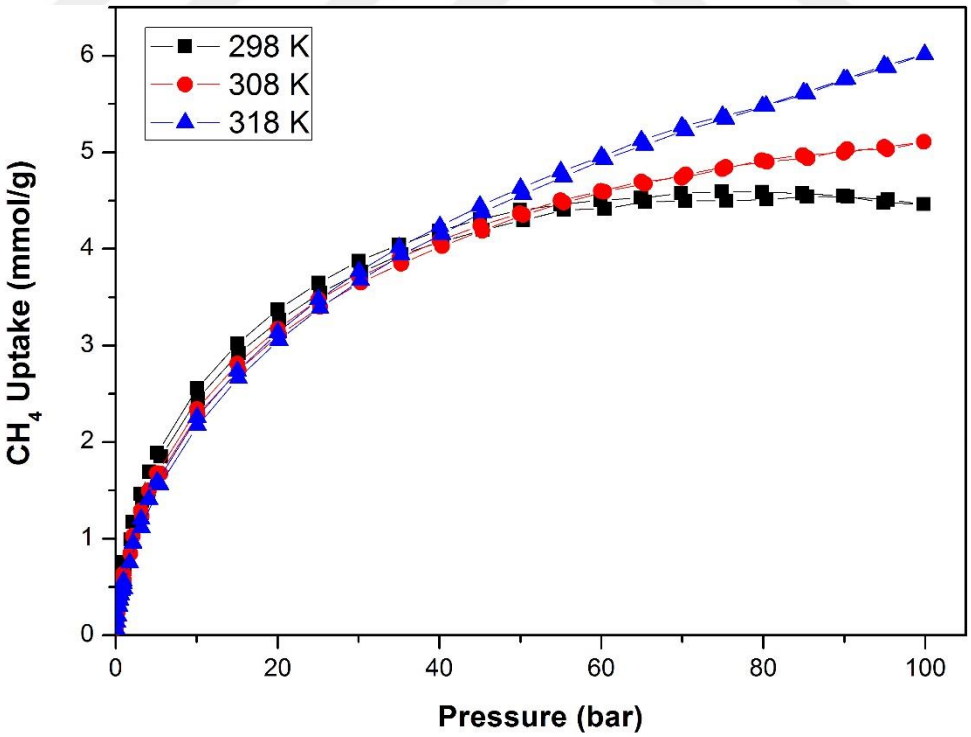

Figure 41. Excess CH_4 Adsorption and Desorption Isotherms for Carbon Aerogel

Adsorption is reversible and reproducible for all aerogels and the amount adsorbed increases with pressure before reaching the maximum. Adsorption amounts decrease with increase in temperature confirming the physical nature of the adsorption process. However, in the isotherms for silica and carbon aerogel, crossovers are observed. In the silica aerogel, isotherm at 318 K crosses isotherm at 308 K at a pressure around 60 bar. On the other hand, in the carbon aerogel there is crossover for all isotherms and as the temperature increases, crossover is observed at lower pressure.

Crossover phenomenon is common in Gibbs excess adsorption isotherms and has not been explored in detail in the literature. Only mathematical models have been used to explain the crossover phenomenon in which differences in the mathematical terms are compared such as using the dual-site Langmuir model [62]. However, it should be noted that the crossover phenomenon is frequently observed for adsorption of supercritical gases [53, 62]. To better understand this phenomenon, it is important to take into consideration the competing effects of both temperature and pressure at especially high pressures. As temperature increases, excess amount adsorbed decreases but at high pressures excess amount adsorbed increases in the case of silica aerogel and carbon aerogel. This is because at high pressures, bulk fluid in the pores increases which could increase the volume of the adsorbed phase due to fluid adsorbing in the hardly accessible sites. The pressure effect dominates the temperature effect and the uptake therefore increases instead of decreasing. Crossover is also observable when the CH_4 uptake is plotted as a function of density of the fluid phase because of the linear relationship between pressure and density of methane above supercritical temperature.

4.2.3. Excess and Absolute Adsorption Isotherms

Absolute adsorption amounts were calculated from experimentally measured excess adsorption amounts by considering the amount of bulk fluid in the pores of the aerogel and not in the adsorbed phase. Figures 42-45 show excess and absolute adsorption isotherms at 298 K, 308 K and 318 K for silica aerogel, RFA-10, RFA-17 and carbon aerogel, respectively.

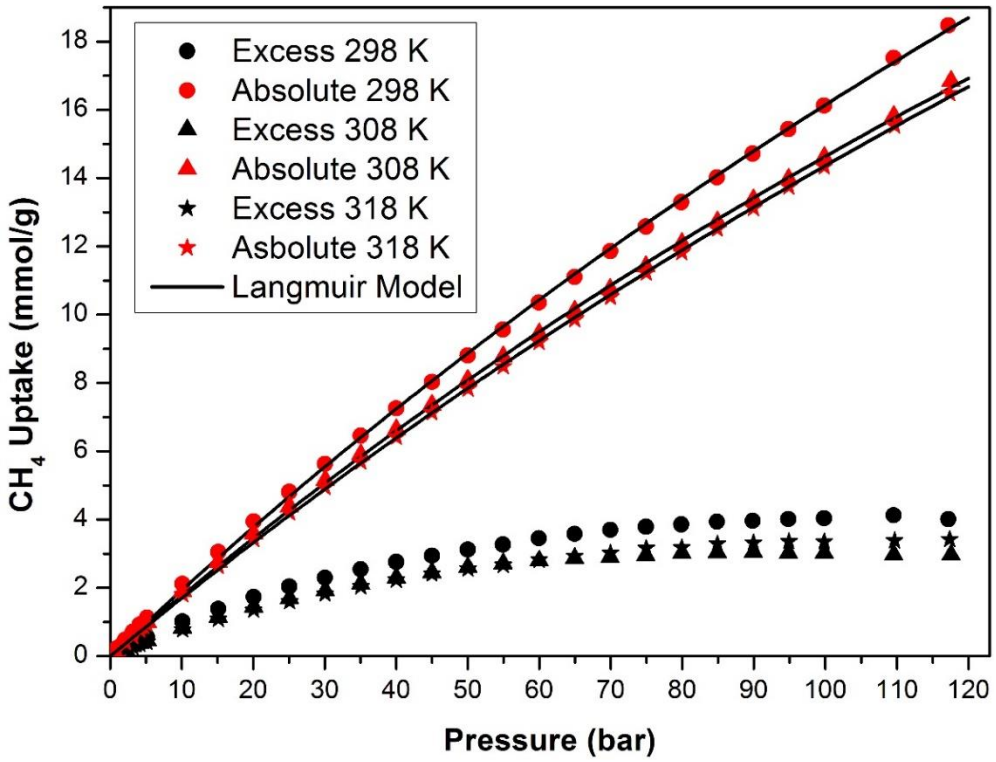

Figure 42. Excess and Absolute Adsorption Isotherms for Silica Aerogel

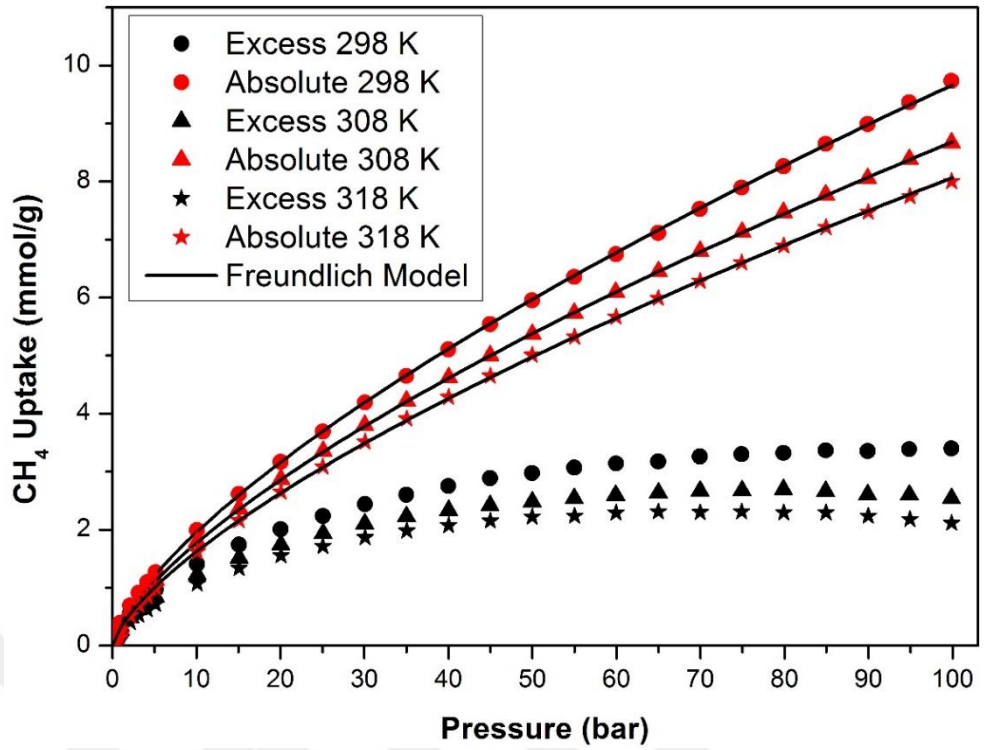

Figure 43. Excess and Absolute Adsorption Isotherms for RFA-10

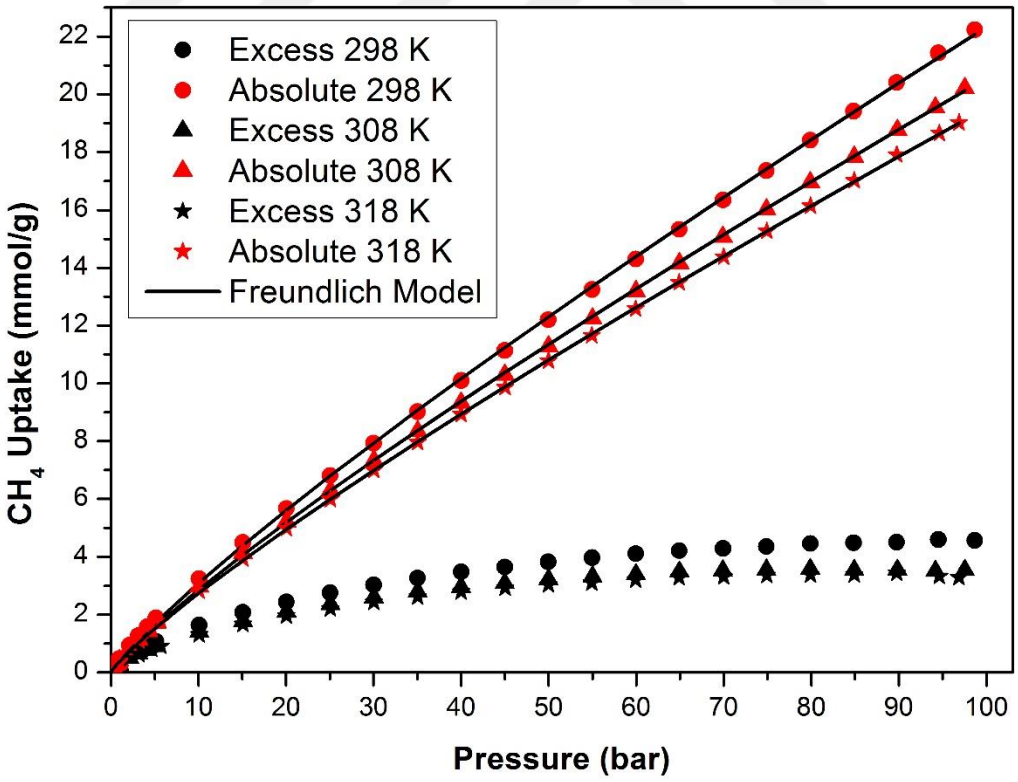

Figure 44. Excess and Absolute Adsorption Isotherms for RFA-17

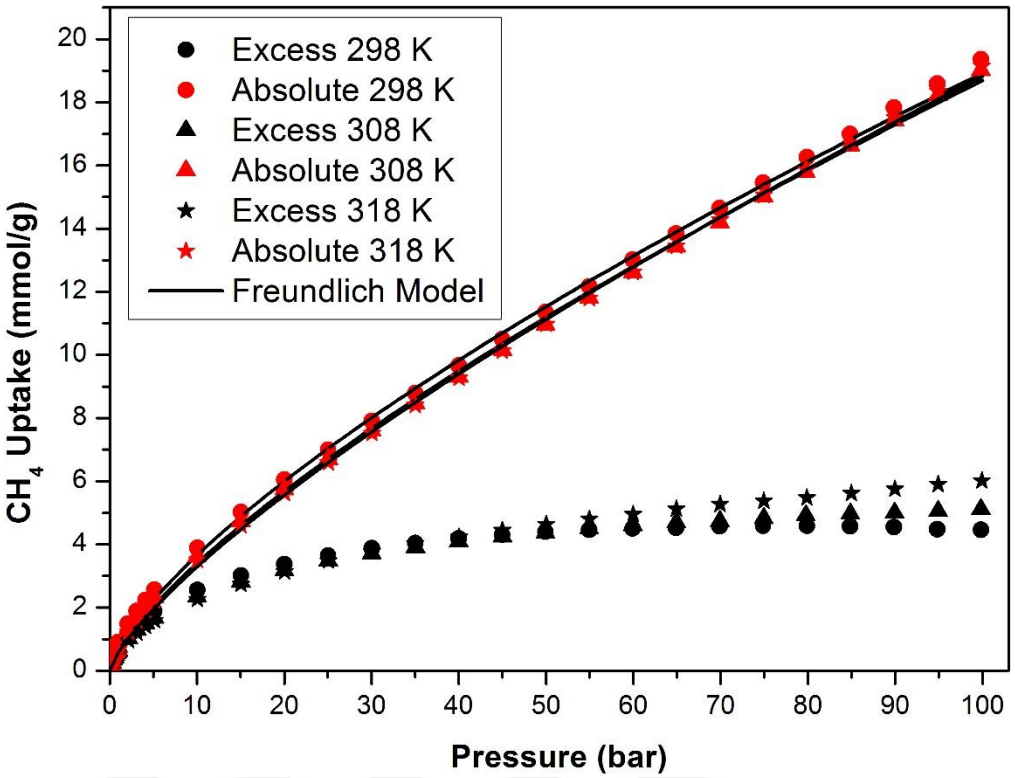

Figure 45. Excess and Absolute Adsorption Isotherms for Carbon Aerogel

All isotherms are classified as type I and absolute uptake at each pressure decreases with increase in temperature for all aerogels which also indicates that the adsorption is physical and exothermic [49, 56, 57]. Crossover phenomenon is not observed in the absolute adsorption isotherms due to the high density of bulk fluid in the pores and the second term in equation 7 dominates.

Since the difference between the absolute and excess adsorbed amount is dependent on the pore volume of the adsorbent, it is found that there is a significant difference between two quantities at all pressures. For silica aerogel, the difference is more than 100% at 1 bar and is more than 150% at pressures greater than 50 bar. Similarly, for RFA-10, the difference is 15% at 1 bar and is more than 100% at pressures greater than 50 bar. For RFA-17, the difference is 40% at 1 bar and is more than 200% at pressures greater than 50 bar. Finally, the difference for carbon aerogel is 20% at 1 bar and is more than 130% at pressures greater than 50 bar. The differences among aerogels

are due to the differences in pore volumes of aerogels which were given in Table 4. Silica aerogel, RFA-17 and carbon aerogel have high pore volumes which result in larger difference between total and excess adsorbed amounts. RFA-10 has low pore volume which leads to smaller difference in the total and excess adsorbed amounts.

Moreover, for aerogels excess adsorbed and absolute adsorbed amounts are not nearly equal at low pressures which is generally the case for other adsorbents. For example, excess and absolute adsorbed amounts for HKUST-1 with a BET surface area of 1555 $m^2 g^{-1}$ and pore volume of 0.71 $cm^3 g^{-1}$ were nearly equal up to pressures of almost 20 bar [53].

4.2.4. Comparison with Other Adsorbents

In order to evaluate aerogels' potential as adsorbents for methane storage in vehicles, it is important to compare the absolute adsorption capacities with other frequently investigated adsorbents such as MOFs and activated carbon. Figure 46 provides comparsion of CH_4 uptake of aerogels with activated carbon [63], HKUST-1 [4], ZIF-8 [51] and several other MOFs [52] at a temperature of 298 K and 35 bar.

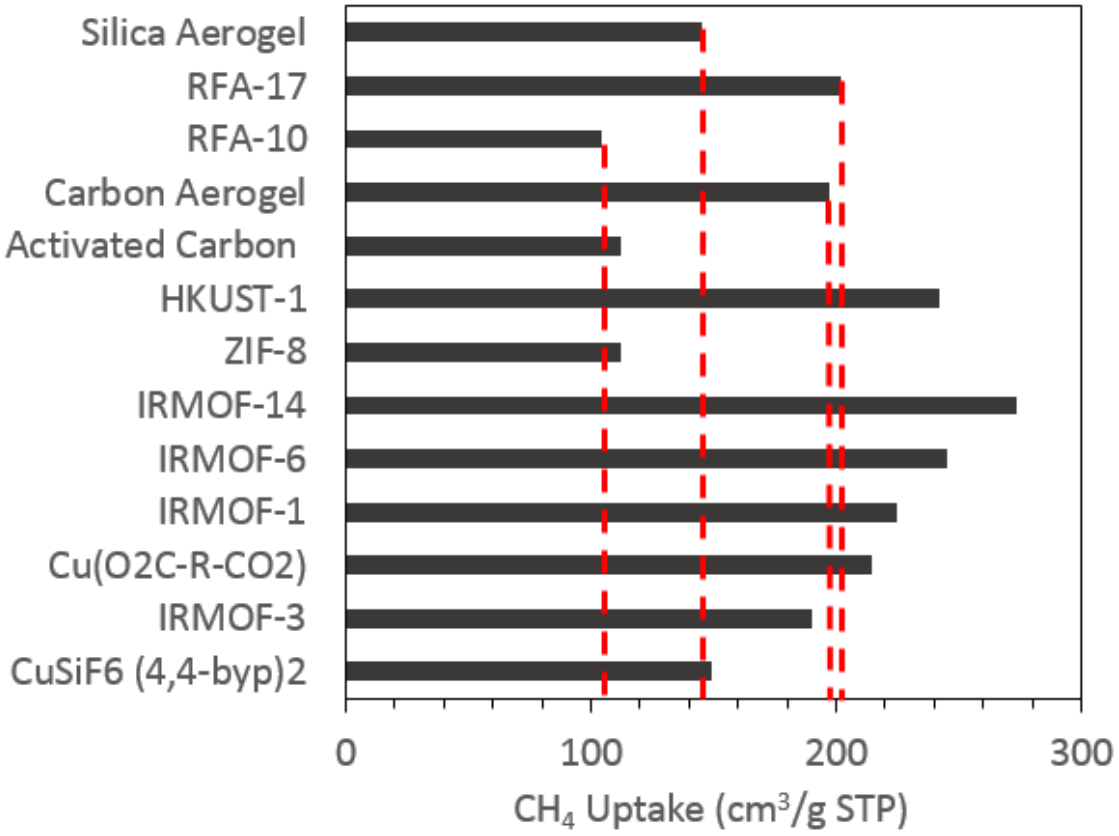

Figure 46. Comparsion of CH_4 Uptake of Aerogels with Other Adsorbents

The results indicate that at a specific temperature and pressure, aerogels have CH_4 uptakes similar and greater than some of the MOFs and activated carbon. Since properties like surface area and pore volumes are tunable for aerogels, it is possible to synthesize aerogels which would have high CH_4 uptakes and they could be potential adsorbents for methane storage in vehicles at safe operating conditions.

4.2.5. Isotherm Fitting

Figures 42 to 45 also show that Langmuir isotherm model fitted the absolute adsorption data well for silica aerogel and Freundlich model was a good fit for resorcinol-formaldehyde and carbon aerogels. This indicates that the surface of silica aerogel could be considered as homogenous. On the other hand, a good Freundlich fit for resorcinol-formaldehyde and carbon aerogels reflects the heterogenity in the surface of aerogels.

Isotherm parameters for absolute adsorption isotherms were also determined from nonlinear fitting at all temperatures and are provided in Table 5.

Table 5. Langmuir and Freundlich Parameters for All Aerogels

Temperature (K)	**298**			**308**			**318**		
Freundlich Parameters	K_f	n	R^2	K_f	n	R^2	K_f	n	R^2
RFA-10	0.3948	1.440	0.9999	0.3603	1.447	1.000	0.3259	1.435	0.9999
RFA-17	0.4272	1.164	0.9999	0.3987	1.168	1.000	0.3838	1.172	1.000
Carbon Aerogel	0.7052	1.400	0.9991	0.6185	1.351	0.9993	0.5734	1.319	0.9995
Langmuir Parameters	K (bar^{-1})	q_m (mmol g^{-1})	R^2	K (bar^{-1})	q_m (mmol g^{-1})	R^2	K (bar^{-1})	q_m (mmol g^{-1})	R^2
Silica Aerogel	0.002195	89.71	0.9998	0.002335	77.33	0.9998	0.002025	85.32	0.9999

4.2.6. Isosteric Heat of Adsorption

Excess adsorption isotherms measured at temperatures of 298, 308 K and 318 K for all aerogels were used to determine isosteric heat of adsorption ,Qst. It is an important thermodynamic quantity because it can provide information on whether the adsorption is physical or chemical as well on the strength of adsorbate-adsorbent interactions [23]. According to the Clausius-Clapeyron equation 5, plots of lnP against 1/T at a constant uptake were created for all aerogels and are shown in Figures 47-50.

The slopes of the lnP versus 1/T plots were used to calculate Qst at different uptakes and the dependence on uptake is provided in Figure 51.

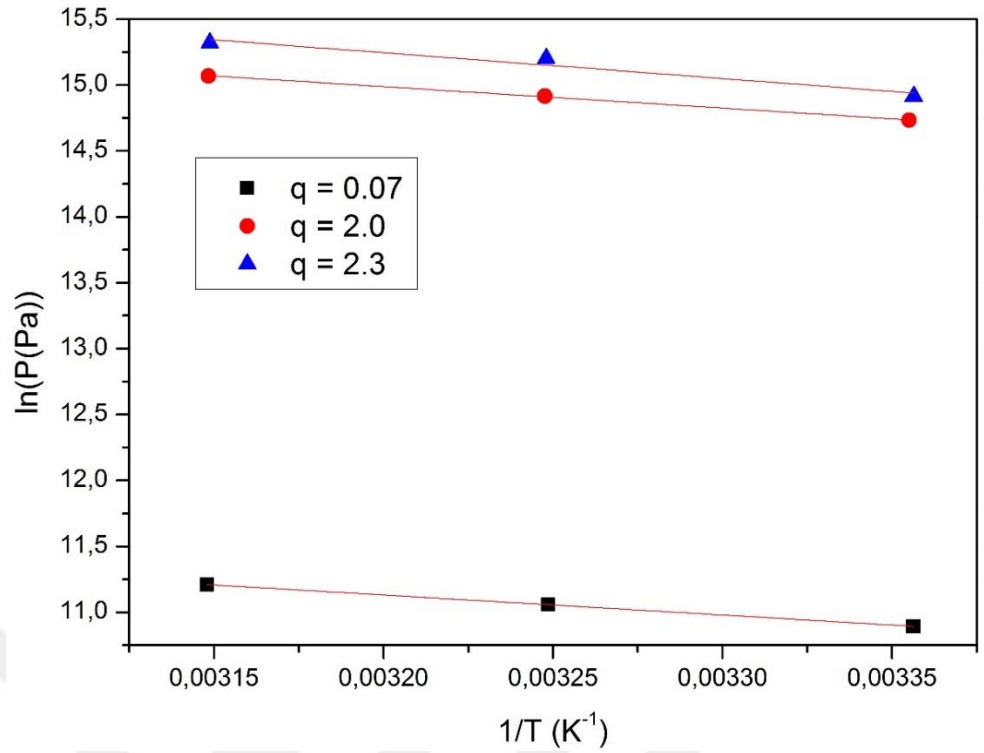

Figure 47. Relationship between lnP and 1/T for Silica Aerogel

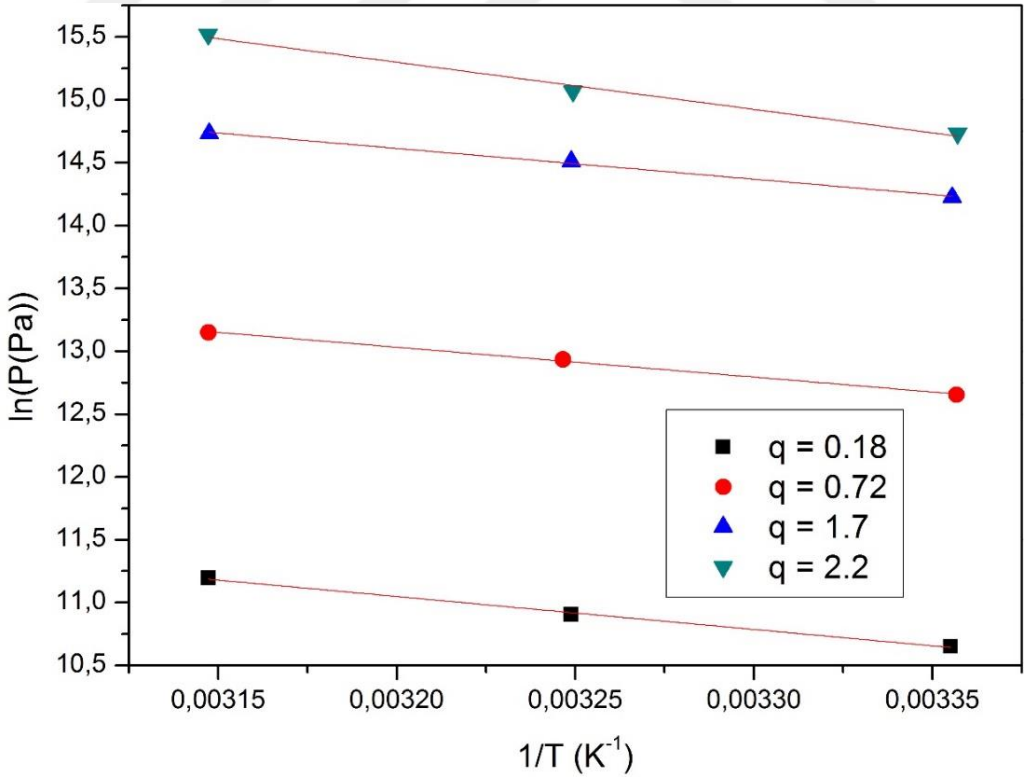

Figure 48. Relationship between lnP and 1/T for RFA-10

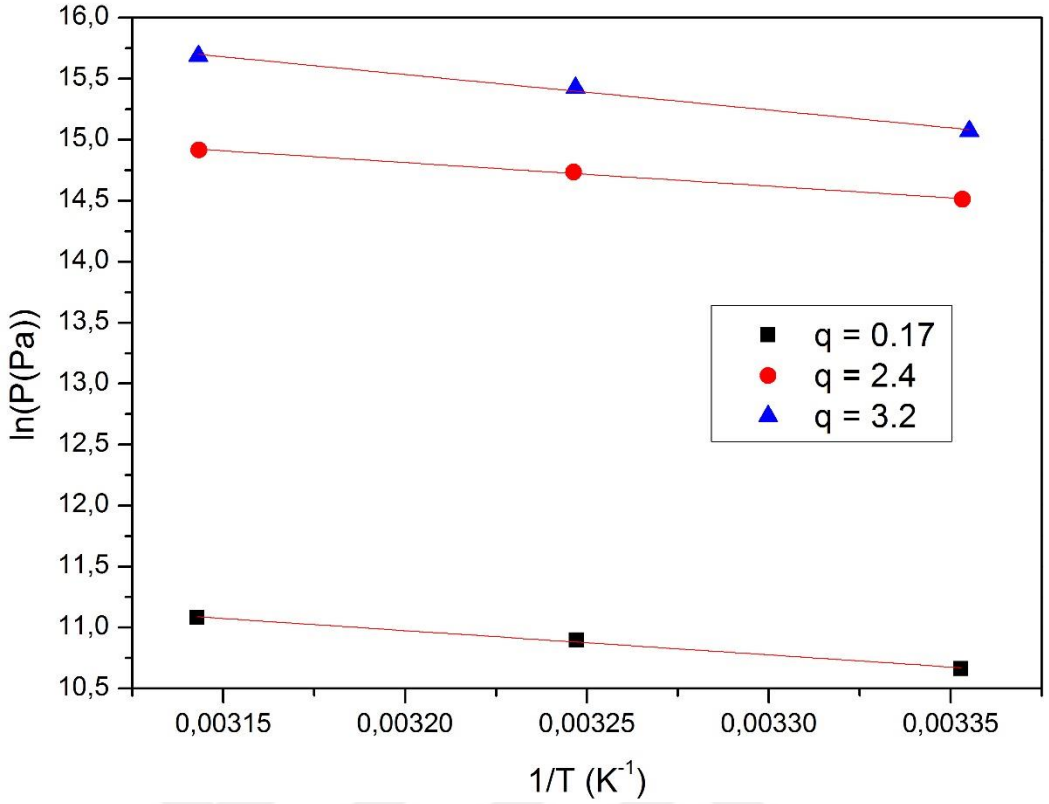

Figure 49. Relationship between lnP and 1/T for RFA-17

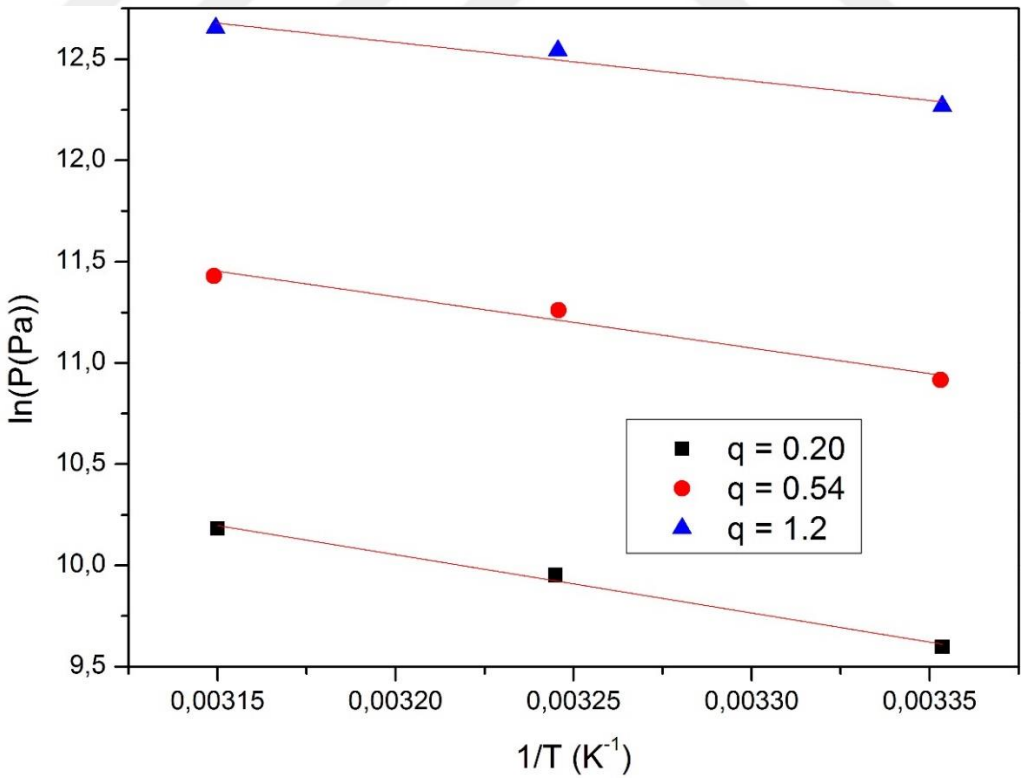

Figure 50. Relationship between lnP and 1/T for Carbon Aerogel

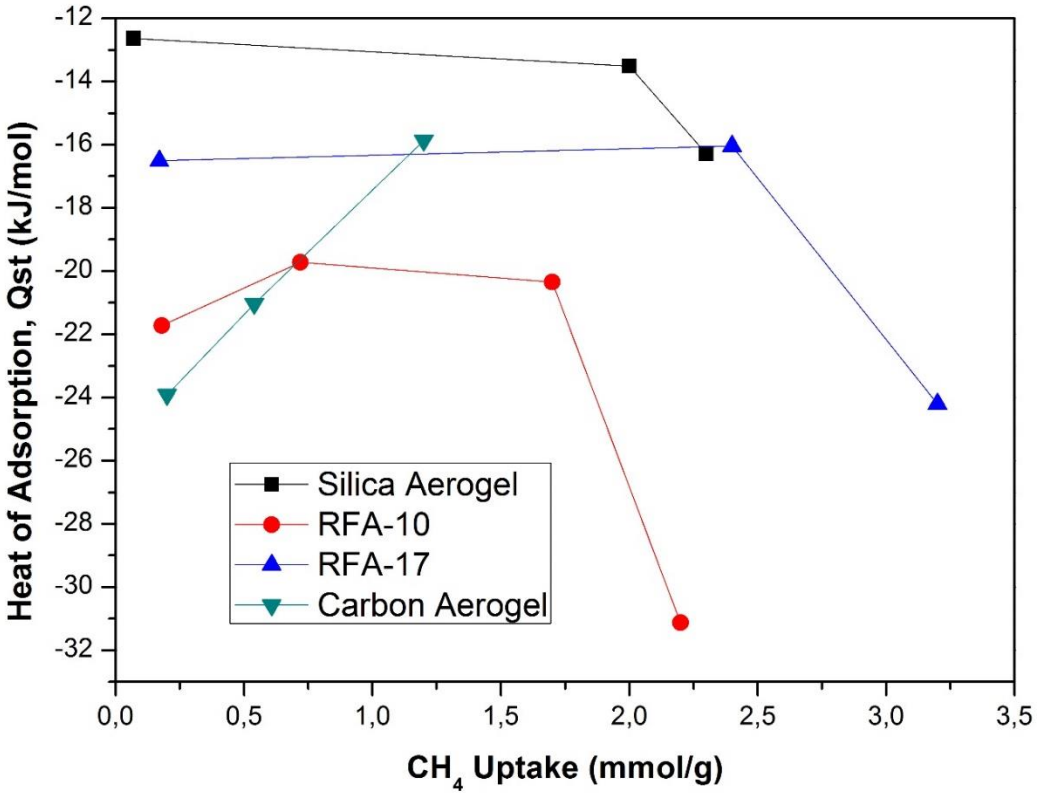

Figure 51. Variation of Heat of Adsorption with CH_4 Uptake for Different Aerogels

It can be seen from Figure 51 that Qst values are dependent on the CH_4 uptake. Values are lower at low uptakes and increases with increase in uptake for silica and RFA-17. Values decrease for carbon aerogel and first increase and then decrease for RFA-10. Negative values confirms the exothermicity of the adsorption process and smaller values of less than 50 kJ/mol show that the adsorption is physical. The higher the value of Qst, the stronger is the interaction of CH_4 with the aerogel. The high values for resorcinol-formaldehyde aerogel with pore size of 10 nm (RFA-10) among all aerogels investigated in this study indicate the strongest interaction of CH_4 molecules with surface active sites. Heat of adsorption could also be higher due to smaller pores [64] and this is also confirmed by observing the trend for carbon aerogel. The Qst is higher at low uptakes because of the adsorption in micropores and decrease with increase in uptake because of the adsorption in bigger sized pores.

The low values for silica aerogel are indicative of weak interaction of CH_4 with surface active sites and is comparable with the values in the range of 8-20 kJ/mol reported for silica based materials such as MCM-41 and silicalite [64]. The range of Qst values for carbon aerogel are also comparable with other carbon based adsorbents such as carbon nanotubes (CNTs) and activated carbons which have Qst values reported in the range of 14-20 kJ/mol [63, 64]. Heat of adsorption of CH_4 on resocinol-formaldehyde aerogel is reported for the first time in this study. In addition to obtaining information about the energetic interaction between the adsorbent and adsorbate from Qst, this parameter is also useful in determining the energy requirement for regeneration of adsorbents which is crucial in the development of technology employing adsorbed methane as fuel in vehicles.

4.3. Kinetics of Adsorption

It is also important to explore kinetics of adsorption in order to understand the mechanism of adsorption as well as getting information about the duration of the process for efficient design of systems. In the volumetric adsorption technique, pressure versus time relationships could be obtained and the experimental data could be fitted with relevant kinetic models to obtain rate constants and mass transfer coefficients. Several kinetic models such as unipore model [65], diffusion model [66] and pseudo first and second order models [67] have been applied to adsorption. X Tang et al. [68] investigated kinetics of high pressure carbon dioxide adsorption on coal by measuring uptakes as function of time. Adsorption process was determined to be controlled by both bulk diffusion and surface interaction with the latter dominating the process. Similarly, Delavar et al. [69] was able to successfully fit pseudo-first-order kinetic model and intra-particle diffusion model to the experimental data of high pressure natural gas adsorption on carbon nanotube and the kinetics of this process was also dominated by surface interactions.

In the volumetric technique used in this study, it was determined that only surface interaction controlled the kinetics and both inter and intra-particle diffusion were not present during the adsorption of CO_2 and CH_4. It is due to the fact that as the adsorbate is expanded into the adsorption chamber, the pressure is same everywhere instantaneously in the chamber including the pores of the adsorbent. Therefore, the pressure change with time data obtained is only associated with the physical adsorption taking place at the surface. The surface interaction-controlled kinetics indicates fast adsorption reaction which is also confirmed by the sufficiently small equilibrium time of 10 minutes.

5. CONCLUSION

Silica, resorcinol-formaldehyde, carbon and wheat starch aerogels were synthesized in this study and excess carbon dioxide and methane adsorption isotherms were measured using a high pressure volumetric technique. The purpose of this work was to evaluate aerogels' potential as adsorbents for carbon dioxide capture and methane storage by investigating adsorption thermodynamics. Total or absolute adsorption was calculated from excess adsorption by considering the amount of bulk fluid in the pores. The total amount was found to differ significantly at all pressures from the excess amount due to high pore volumes of aerogels. Silica aerogel had maximum absolute CO_2 adsorption uptake of 14 mmol/g at 308 K and 35 bar and resorcinol-formaldehyde aerogel (RFA) had maximum absolute CH_4 adsorption uptake of 22 mmol/g at 298 K and 100 bar.

Excess CO_2 uptakes were found to be proportional to the mesopore surface area of aerogels while micropore surface area had a significant effect in the uptakes of methane. Isosteric heats of adsorption, Qst, were also calculated to get insight into adsorbent-adsorbate interactions. Qst values were dependent on the uptake, however, wheat starch aerogel had highest heats of CO_2 adsorption and RFA had highest heats of CH_4 adsorption.

The results obtained were also comparable with other commonly investigated adsorbents such as activated carbons and metal organic frameworks and open up new opportunity to investigate native and modified aerogels as potential carbon dioxide capture and methane storage materials.

REFERENCES

1. (EIA), U.S.E.I.A., *International Energy Outlook 2016*. 2016, U.S. Department of Energy: Washington. p. 1-290.
2. Yang, H.Q., Xu, Z. H., Fan, M. H., Gupta, R., Slimane, R. B., Bland, A. E., Wright, I., *Progress in carbon dioxide separation and capture: A review.* Journal of Environmental Sciences, 2008. **20**(1): p. 14-27.
3. D'Alessandro, D.M., Smit, B., Long, J. R., *Carbon dioxide capture: prospects for new materials.* Angew Chem Int Ed Engl, 2010. **49**(35): p. 6058-82.
4. Mirian Elizabeth Casco, M.M.-E., Enrique Gadea-Ramos, Katsumi Kaneko, Joaquín Silvestre-Albero, Francisco Rodríguez-Reinoso, *High-Pressure Methane Storage in Porous Materials: Are Carbon Materials in the Pole Position?* Chemistry of Materials, 2015. **27**: p. 959-964.
5. Wormeyer, K., Alnaief, M., Smirnova, I., *Amino functionalised Silica-Aerogels for CO2-adsorption at low partial pressure.* Adsorption-Journal of the International Adsorption Society, 2012. **18**(3-4): p. 163-171.
6. Ulker, Z. and C. Erkey, *An emerging platform for drug delivery: Aerogel based systems.* Journal of Controlled Release, 2014. **177**: p. 51-63.
7. Slejko, F.L., *Adsorption technology: A step-by-step approach to process evaluation and application*. 6 ed. 1985, New York: M. Dekker.
8. Auroux, A., *Special Issue: Calorimetry and Thermal Effects in Catalysis Preface.* Thermochimica Acta, 2013. **567**: p. V-V.
9. R.T.Yang, *Gas Separation by Adsorption Process*. 1997, London: Imperial College Press.
10. Ruthven, D.M., *Principles of Adsorption and Adsorption Processes*. 1984, United States of America: John Wiley & Sons, Inc.
11. Brunauer, S., *The Adsorption of Gases and Vapours*. 1945, Oxford: Oxford University Press.
12. Thommes, S.L.J.E.S.M.A.T.M., *Characterization of Porous Solids and Powders: Surface Area, Pore Size and Density*. 2004, Netherlands: Kluwer Academic Publishers.
13. Sing, K.S.W., Everett, D. H., Haul, R. A. W., Moscou, L., Pierotti, R. A., Rouquerol, J., Siemieniewska, T., *Reporting Physisorption Data for Gas Solid Systems with Special Reference to the Determination of Surface-Area and Porosity (Recommendations 1984).* Pure and Applied Chemistry, 1985. **57**(4): p. 603-619.
14. Lee, D., et al., *Gravimetric analysis of the adsorption and desorption of CO2 on amine-functionalized mesoporous silica mounted on a microcantilever array.* Environ Sci Technol, 2011. **45**(13): p. 5704-9.
15. Watson, G.C., et al., *Volumetric Adsorption Measurements of N-2, CO2, CH4, and a CO2 + CH4 Mixture on a Natural Chabazite from (5 to 3000) kPa.* Journal of Chemical and Engineering Data, 2012. **57**(1): p. 93-101.
16. Garrone, E., et al., *Thermodynamics of CO adsorption on the zeolite Na-ZSM-5 - A combined microcalorimetric and FTIR spectroscopic study.* Physical Chemistry Chemical Physics, 1999. **1**(4): p. 513-518.
17. Ndjaka, J.M.B., et al., *Molecular simulations of adsorption isotherms of small alkanes in FER-, TON-, MTW- and DON-type zeolites.* Microporous and Mesoporous Materials, 2004. **68**(1-3): p. 37-43.
18. *Adsorption Measurement Technique*. Available from: http://www.jinaipu.com/UpFile/20150821104208.pdf.

19. Langmuir, I., *The Adsorption Of Gases On Plane Surfaces Of Glass, Mica And Platinum.* American Chemical Society, 1918. **40**(9): p. 1361-1403.
20. Bolis, V., *Fundamentals in Adsorption at the Solid-Gas Interface. Concepts and Thermodynamics*, in *Calorimetry and Thermal Methods in Catalysis*, A. Auroux, Editor. 2013, Springer.
21. Stephen Brunauer., P.H.E., Edward Teller, *Adsorption of Gases in Multimolecular Layers.* American Chemical Society, 1938. **60**(2): p. 309-319.
22. Gary Attard., C.B., *Surfaces*. 1998, Oxford: Oxford Chemistry Primers.
23. Julian Szekely, J.W.E., Hong Yong Sohn, *Gas-solid Reactions*. 1976, New York: Academic Press, Inc.
24. K. Wörmeyer, I.S., *Breakthrough measurements of CO2 through aminofunctionalised aerogel adsorbent at low partial pressure: Experiment and modeling.* Microporous and Mesoporous Materials, 2014. **184**: p. 61-69.
25. Myers, A.L., Monson, P. A., *Physical adsorption of gases: the case for absolute adsorption as the basis for thermodynamic analysis.* Adsorption-Journal of the International Adsorption Society, 2014. **20**(4): p. 591-622.
26. Dunne, J.A., et al., *Calorimetric heats of adsorption and adsorption isotherms .2. O-2, N-2, Ar, CO2, CH4, C2H6, and SF6 on NaX, H-ZSM-5, and Na-ZSM-5 zeolites.* Langmuir, 1996. **12**(24): p. 5896-5904.
27. Humayun, R., Tomasko, D. L., *High-resolution adsorption isotherms of supercritical carbon dioxide on activated carbon.* Aiche Journal, 2000. **46**(10): p. 2065-2075.
28. Mohammad Songolzadeh, M.T.R., Mansooreh Soleimani., *Carbon Dioxide Capture and Storage: A General Review on Adsorbents.* International Journal of Chemical, Molecular, Nuclear, Materials and Metallurgical Engineering, 2012. **6**(10): p. 900-907.
29. Cui, S., Cheng, W. W., Shen, X. D., Fan, M. H., Russell, A., Wu, Z. W., Yi, X. B., *Mesoporous amine-modified SiO2 aerogel: a potential CO2 sorbent.* Energy & Environmental Science, 2011. **4**(6): p. 2070-2074.
30. S.S.Kistler, *Coherent Expanded Aerogels and Jellies.* Nature, 1931. **127**: p. 741.
31. Dorcheh, A.S. and M.H. Abbasi, *Silica aerogel; synthesis, properties and characterization.* Journal of Materials Processing Technology, 2008. **199**(1-3): p. 10-26.
32. Sanli, D. and C. Erkey, *Effect of polymer molecular weight and deposition temperature on the properties of silica aerogel/hydroxy-terminated poly(dimethylsiloxane) nanocomposites prepared by reactive supercritical deposition.* Journal of Supercritical Fluids, 2015. **105**: p. 99-107.
33. Pekala, R.W., *Organic Aerogels from the Polycondensation of Resorcinol with Formaldehyde.* Journal of Materials Science, 1989. **24**(9): p. 3221-3227.
34. Mulik, S., Sotiriou-Leventis, Chariklia, *Resorcinol–Formaldehyde Aerogels*, in *Aerogels Handbook*, M.A. Aegerter, Leventis, Nicholas., Koebel, Matthias M., Editor. 2011, Springer New York: New York, NY. p. 215-234.
35. Al-Muhtaseb, S.A. and J.A. Ritter, *Preparation and properties of resorcinol-formaldehyde organic and carbon gels.* Advanced Materials, 2003. **15**(2): p. 101-+.
36. Lin, C., J.A. Ritter, and B.N. Popov, *Correlation of double-layer capacitance with the pore structure of sol-gel derived carbon xerogels.* Journal of the Electrochemical Society, 1999. **146**(10): p. 3639-3643.
37. Tamaki, Y., T. Konishi, and M. Tako, *Gelation and Retrogradation Mechanism of Wheat Amylose.* Materials, 2011. **4**(10): p. 1763-1775.

38. Ali Ubeyitogullari., O.N.C., *Formation of nanoporous aerogels from wheat starch.* Carbohydrate Polymers, 2016. **147**: p. 125-132.
39. Glenn, G.M. and D.W. Irving, *Starch-Based Microcellular Foams.* Cereal Chemistry, 1995. **72**(2): p. 155-161.
40. De Marco, I., Baldino, L., Cardea, S., Reverchon, E., *Supercritical Gel Drying for the Production of Starch Aerogels for Delivery Systems.* Icheap12: 12th International Conference on Chemical & Process Engineering, 2015. **43**: p. 307-312.
41. Eric Sundquist, R.B., Stephen Faulkner, Robert Gleason, Jennifer Harden, Yousif Kharaka, Larry Tieszen, Mark Waldrop., *Carbon Sequestration to Mitigate Climate Change*, U.S.D.o.t. Interior, Editor. 2008, United States Geological Survey: USA. p. 1-4.
42. Siriwardane, R.V., Shen, M. S., Fisher, E. P., Poston, J. A., *Adsorption of CO2 on molecular sieves and activated carbon.* Energy & Fuels, 2001. **15**(2): p. 279-284.
43. Cavenati, S., Grande, C. A., Rodrigues, A. E., *Adsorption equilibrium of methane, carbon dioxide, and nitrogen on zeolite 13X at high pressures.* Journal of Chemical and Engineering Data, 2004. **49**(4): p. 1095-1101.
44. Millward, A.R., Yaghi, O. M., *Metal-organic frameworks with exceptionally high capacity for storage of carbon dioxide at room temperature.* Journal of the American Chemical Society, 2005. **127**(51): p. 17998-17999.
45. Kong, Y., Jiang, G., Fan, M., Shen, X., Cui, S., Russell, A. G., *A new aerogel based CO2 adsorbent developed using a simple sol-gel method along with supercritical drying.* Chem Commun (Camb), 2014. **50**(81): p. 12158-61.
46. Linneen, N., Pfeffer, R., Lin, Y. S., *CO2 capture using particulate silica aerogel immobilized with tetraethylenepentamine.* Microporous and Mesoporous Materials, 2013. **176**: p. 123-131.
47. Wang, Z., Dai, Z., Wu, J. J., Zhao, N., Xu, J., *Vacuum-Dried Robust Bridged Silsesquioxane Aerogels.* Advanced Materials, 2013. **25**(32): p. 4494-4497.
48. Masika, E., Mokaya, R., *High surface area metal salt templated carbon aerogels via a simple subcritical drying route: preparation and CO2 uptake properties.* Rsc Advances, 2013. **3**(39): p. 17677-17681.
49. Alhwaige, A.A., Ishida, H., Qutubuddin, S., *Carbon Aerogels with Excellent CO2 Adsorption Capacity Synthesized from Clay-Reinforced Biobased Chitosan-Polybenzoxazine Nanocomposites.* Acs Sustainable Chemistry & Engineering, 2016. **4**(3): p. 1286-1295.
50. Alhwaige, A.A., Agag, T., Ishida, H.,Qutubuddin, S., *Biobased chitosan hybrid aerogels with superior adsorption: Role of graphene oxide in CO2 capture.* Rsc Advances, 2013. **3**(36): p. 16011-16020.
51. Zhou, W., et al., *Hydrogen and methane adsorption in metal-organic frameworks: A high-pressure volumetric study.* Journal of Physical Chemistry C, 2007. **111**(44): p. 16131-16137.
52. Irena Senkovska, S.K., *High pressure methane adsorption in the metal-organic frameworks Cu3(btc)2, Zn2(bdc)2dabco, and Cr3F(H2O)2O(bdc)3.* Microporous and Mesoporous Materials, 2008. **112**: p. 108-115.
53. J. Moellmer., A.M., F. Dreisbach., R. Glaeser., R. Staudt d, *High pressure adsorption of hydrogen, nitrogen, carbon dioxide and methane on the metal–organic framework HKUST-1.* Microporous and Mesoporous Materials, 2011. **138**: p. 140-148.
54. *Thermophysical properties of carbon dioxide and methane*, in *NIST Chemistry WebBook*. 2016, National Institute of Standards and Technology.

55. Menon, P.G., *Adsorption at high pressures.* Chemical Reviews, 1968. **68**(3): p. 277-294.
56. Chitrakshi Goela, H.K., Haripada Bhuniaa, Pramod K. Bajpaia, *Carbon dioxide adsorption on nitrogen enriched carbon adsorbents: Experimental, kinetics, isothermal and thermodynamic studies.* Journal of CO2 Utilization, 2016. **16**: p. 50-63.
57. Hao, G.P., Li, W. C., Qian, D., Lu, A. H., *Rapid synthesis of nitrogen-doped porous carbon monolith for CO2 capture.* Adv Mater, 2010. **22**(7): p. 853-7.
58. Bidyut Baran Saha, S.J., Shigeru Koyama, Ibrahim I. El-Sharkawy., *Carbon Dioxide Adsorption Isotherms on Activated Carbons.* Journal of Chemical and Engineering Data, 2011. **56**: p. 1974-1981.
59. Youssef Belmabkhout, A.S., *Effect of pore expansion and amine functionalization of mesoporous silica on CO2 adsorption over a wide range of conditions.* Adsorption, 2009. **15**: p. 318-328.
60. Tang, X., et al., *Thermodynamic analysis of high pressure methane adsorption in Longmaxi shale.* Fuel, 2017. **193**: p. 411-418.
61. Alcaniz-Monge, J., Lozano-Castello, D.,Cazorla-Amoros, D.,Linares-Solano, A., *Fundamentals of methane adsorption in microporous carbons.* Microporous and Mesoporous Materials, 2009. **124**(1-3): p. 110-116.
62. Tang, X., et al., *A dual-site Langmuir equation for accurate estimation of high pressure deep shale gas resources.* Fuel, 2016. **185**: p. 10-17.
63. Shuji Himeno, T.K., Shoichi Fujita, *High-Pressure Adsorption Equilibria of Methane and Carbon Dioxide on Several Activated Carbons.* Chemical engineering Data, 2005. **50**: p. 369-376.
64. Duren, T., et al., *Design of new materials for methane storage.* Langmuir, 2004. **20**(7): p. 2683-2689.
65. Smith, D.M. and F.L. Williams, *Diffusion-Models for Gas-Production from Coal - Determination of Diffusion Parameters.* Fuel, 1984. **63**(2): p. 256-261.
66. Jian, X., P. Guan, and W. Zhang, *Carbon dioxide sorption and diffusion in coals: Experimental investigation and modeling.* Science China-Earth Sciences, 2012. **55**(4): p. 633-643.
67. Azizian, S., *Kinetic models of sorption: a theoretical analysis.* Journal of Colloid and Interface Science, 2004. **276**(1): p. 47-52.
68. Xu Tang., N.R., Ellen Gilliland, *Isothermal adsorption kinetics properties of carbon dioxide in crushed coal.* Greenhouse Gases: Science and Technology, 2015. **5**: p. 1-15.
69. Maedeh Delavar., A.A.G., Mohsen Jahanshahi., Soodabeh Khalili., Nima Nabian, *Equilibria and kinetics of natural gas adsorption on multi-walled carbon nanotube material.* Rsc Advances, 2012. **2**: p. 4490-4497.